Deep–Sea Research I 181 (2022) 103685

Contents lists available at ScienceDirect

Deep-Sea Research Part I

journal homepage: www.elsevier.com/locate/dsri

Genetic diversity, gene flow and hybridization in fan-shaped sponges (*Phakellia* spp.) in the North-East Atlantic deep sea

Sergi Taboada [a,b,c,*], Pilar Ríos [c,d,e], Alex Mitchell [b], Alex Cranston [b], Kathrin Busch [f], Vanina Tonzo [g], Paco Cárdenas [h], Francisco Sánchez [d], Carlos Leiva [b,i], Vasiliki Koutsouveli [b,f,j], Javier Cristobo [c,e], Joana R. Xavier [k,l], Ute Hentschel [f,m], Hans-Tore Rapp [l,n], Christine Morrow [o], Jim Drewery [p], Pedro E. Romero [q], Maria Belén Arias [b,r], Connie Whiting [s], Ana Riesgo [b,t]

[a] *Departamento de Biodiversidad, Ecología y Evolución, Universidad Complutense de Madrid, Facultad de Ciencias, 28049, Madrid, Spain*
[b] *Life Sciences Department, The Natural History Museum, Cromwell Road, London SW7 5BD, UK*
[c] *Departamento de Ciencias de la Vida, EU-US Marine Biodiversity Group, Universidad de Alcalá, 28871 Alcalá de Henares, Spain*
[d] *Instituto Español de Oceanografía, Centro Oceanográfico de Santander, Promontorio San Martín S/n, Apdo. 240, 39080, Santander, Spain*
[e] *Instituto Español de Oceanografía. Centro Oceanográfico de Gijón, C/ Príncipe de Asturias 70 bis, 33212 Gijón, Asturias, Spain*
[f] *RD3 Marine Symbioses, GEOMAR Helmholtz Centre for Ocean Research Kiel, Kiel, Germany*
[g] *Animal Biodiversity and Evolution Metazoa Phylogenetics Lab, Centro Mediterráneo de Investigaciones Marinas y Ambientales, 08003, Barcelona, Spain*
[h] *Pharmacognosy, Department of Pharmaceutical Biosciences, Uppsala University, BMC, Husargatan 3, Uppsala 75123, Sweden*
[i] *Marine Laboratory, University of Guam, 303 University Drive, Mangilao 96923, Guam, USA*
[j] *Department of Marine Ecology, GEOMAR Helmholtz Centre for Ocean Research Kiel, Düsternbrooker Weg 20, 24105, Kiel, Germany*
[k] *CIIMAR – Interdisciplinary Centre of Marine and Environmental Research of the University of Porto, 4450-208 Matosinhos, Portugal*
[l] *University of Bergen, Department of Biological Sciences, 5006 Bergen, Norway*
[m] *Christian-Albrecht University of Kiel, Kiel, Germany*
[n] *NORCE, Norwegian Research Centre, NORCE Environment, Nygårdsgaten 112, 5008 Bergen, Norway*
[o] *Queen's University Marine Laboratory, Portaferry, Northern Ireland, UK*
[p] *Marine Scotland Science, Marine Laboratory, 375 Victoria Road, Aberdeen, AB11 9DB, UK*
[q] *Departamento de Ciencias Biológicas y Fisiológicas, Facultad de Ciencias y Filosofía. Universidad Peruana Cayetano Heredia. 15102 Lima, Peru*
[r] *School of Life Sciences, University of Essex, Colchester Campus, 3SW 322, UK*
[s] *Cell and Developmental Biology Department, University College London, Rockefeller Building, 21 University Street, London WC1E 6DE, UK*
[t] *Departamento de Biodiversidad y Biología Evolutiva, Museo Nacional de Ciencias Naturales, 28006, Madrid, Spain*

A R T I C L E I N F O

Keywords:
Introgression
SNPs
COI
Microbial community analysis
Conservation
MPA

A B S T R A C T

Deep-sea North Atlantic sponge grounds are crucial components of the marine fauna providing a key role in ecosystem functioning. To properly develop effective conservation and management plans, it is crucial to understand the genetic diversity, molecular connectivity patterns and turnover at the population level of the species involved. Here we present the study of two congeneric sponges, *Phakellia robusta* and *Phakellia hirondellei*, using multiple sources of evidence. Our phylogenetic study using a fragment of *COI* placed these two species as sister. Haplotype network analysis using *COI* revealed no genetic structure for *P. hirondellei* in samples from the Cantabrian Sea (<100 km). Contrastingly, *P. robusta* showed a clear genetic structure separating deep-water samples from the Cantabrian Sea and the Hatton-Rockall Basin, from samples from shallower waters from Kerry Head Reefs, NW of Orkney, and Norway. ddRADseq-derived SNPs for *P. robusta* also segregated samples by bathymetry rather than by geographical distances, and detected a predominant northwards migration for shallow-water specimens connecting sites separated ca. 2,000 km, probably thanks to prevalent oceanographic currents. Importantly, our analysis using SNPs combining the datasets of the two species revealed the presence of potential hybrids, which was corroborated by morphological (spicule) and microbial (*16S* amplicon sequencing) analyses. Our data suggest that hybridization between these two species occurred at least two times in the past. We discuss the importance of using next-generation techniques to unveil hybridization and the implications of our results for conservation.

* Corresponding author. Departamento de Biodiversidad, Ecología y Evolución, Universidad Complutense de Madrid, Facultad de Ciencias, 28049, Madrid, Spain.
E-mail address: sergiotab@gmail.com (S. Taboada).

https://doi.org/10.1016/j.dsr.2021.103685
Received 24 May 2021; Received in revised form 6 December 2021; Accepted 7 December 2021
Available online 22 December 2021
0967-0637/© 2022 The Authors. Published by Elsevier Ltd. This is an open access article under the CC BY-NC-ND license (http://creativecommons.org/licenses/by-nc-nd/4.0/).

1. Introduction

The North Atlantic deep-sea harbours a rich diversity of sponges that can sometimes form dense aggregations of individuals commonly known as sponge grounds (Howell et al., 2016; Maldonado et al., 2017). Sponge grounds, either mono- or multispecific, provide tridimensional structure that can be used by a plethora of organisms, thus substantially increasing the biodiversity and abundance of associated fauna, including not only other marine invertebrates (Beazley et al., 2013), but also fish that frequently recruit and live in these habitats (Kenchington et al., 2013; Pham et al., 2015; Sánchez et al., 2017). The presence of structure-forming sponges also greatly modifies the availability of organic matter by producing large amounts of detritus (Witte, 1996) and by recycling the dissolved organic carbon thanks to the so-called sponge-loop (De Goeij et al., 2013), thus greatly contributing to the bentho-pelagic coupling. Sponges and their associated grounds therefore are not only key to ecosystem functioning but also offer many ecosystem services and, in turn, benefits to humans (Paoli et al., 2017).

As in other marine ecosystems many of the major threats faced by deep-sea sponge grounds are anthropogenic in nature. This mainly involves habitat destruction primarily derived from trawling and bottom-fishing activities (Pham et al., 2019; Roberts, 2002), but also, more recently, other causes have expanded the panoply of threats including industrial activities such as hydrocarbon exploration or deep-sea mining (Wedding et al., 2015). Despite being relatively isolated, deep-sea habitats have also revealed to be highly sensitive to climate change (Hughes and Narayanaswamy, 2013). Climate change will be likely to produce changes in ocean currents and water temperature which might result in cascading effects on organisms in the deep sea, affecting their growth rate, distribution, and reproduction (Hughes and Narayanaswamy, 2013; Sweetman et al., 2017). The aforementioned threats are leading to a decrease in biodiversity and genetic diversity in wild populations, thus prompting decreased resilience to environmental stressors and reducing the adaptive evolutionary potential of the species (Spielman et al., 2004). Consequently, in order to proper develop effective conservation and management plans, it is crucial to understand the genetic diversity, molecular connectivity patterns and turnover at the population level of the species involved (Baco et al., 2016).

Molecular connectivity studies in marine invertebrates from non-chemosynthetic deep-sea habitats are scarce, and there is thus a clear need to extend them to key species from a variety of habitats, life histories, and taxonomic groups across the deep sea (Baco et al., 2016; Taylor and Roterman, 2017). Deep-water populations are normally well connected over large geographical distances (100s–1000s of km) at similar depths. Generally, it is differences in depth (100s–1000s of m) which explain the variation in genetic structure observed among populations (see Taylor and Roterman 2017). This prevalent pattern of vertical divergence being stronger than horizontal, aided by the difficulties of larvae and/or adults to perform vertical migrations (Young et al., 1996), might cause a restriction (or even disruption) of gene flow leading to allopatric populations and the subsequent emergence of cryptic species (e.g. France and Kocher 1996; Quattro et al., 2001; Zardus et al., 2006; Schüller 2011).

As evidenced in a recent review by Taylor and Roterman (2017), most of the studies on the connectivity of deep-water species have used either traditional markers and/or microsatellites, which have proved to be very useful to detect genetic structure in some cases but may have clear limitations in others. For instance, the mitochondrial cytochrome *c* oxidase subunit I (*COI*), commonly used for demographic studies in marine invertebrates, generally provides little or no resolution for both shallow- and deep-water sponges (see Pérez-Portela and Riesgo 2018; Taboada et al., 2018). This has led to the use of highly polymorphic microsatellites for sponges, which have shown to be very efficient at detecting gene flow among sampling sites, even at small scales (see Pérez-Portela and Riesgo 2018; Riesgo et al., 2019). Despite the proven efficiency of microsatellites for population genetics studies in deep-water organisms, there is a need to explore new molecular techniques using single nucleotide polymorphisms (SNPs) generated from reduced representation genome studies that can be easily applied to non-model organisms at relatively low costs (Taylor and Roterman 2017). This is particularly true for techniques such as double-digest Restriction site-Associated DNA Sequencing (ddRADseq), able to generate 100s–1000s of SNPs, providing not only the power to perform fine-scale population genomics studies, but also to investigate phylogenomics, adaptation strategies, or introgression, among others (see Andrews et al., 2016). Despite studies using SNPs gaining interest in regards to the use of microsatellites (Hohenlohe et al., 2018), this approach has only been applied in a limited number of occasions in marine invertebrates (e.g. Bouchemousse et al., 2016; Fraïsse et al., 2016; Galaska et al., 2017; Breusing et al., 2019; Leiva et al., 2019) and, to our knowledge, only twice for deep-water sponge species (Brown et al., 2017; Busch et al., 2020).

Here we present the study case of two deep-sea demosponges of the genus *Phakellia* (order Bubarida, family Bubaridae): *Phakellia robusta* Bowerbank, 1866 and *Phakellia hirondellei* Topsent (1890). In the deep sea, *Phakellia* spp. are key species in North-Atlantic sponge grounds, providing a high environmental conservation value to the areas where they occur since they are considered members of the habitat type 1170-Reefs according to the Habitats Directive of the European Union (EC, 2013). *Phakellia* spp. grounds are abundant in the North Atlantic and also host a wide variety of epifaunal communities (Klitgaard, 1995). While *Phakellia robusta* is distributed from the Azores to the boreo-Arctic, with some populations reported in the Mediterranean Sea, *Phakellia hirondellei* is restricted to the coasts of the Iberian Peninsula, the Macaronesia and the Gulf of Lion (Boury-Esnault et al., 1994; Fourt et al., 2017; Santín et al., 2018; Topsent, 1890, 1928; Uriz, 1984). Recently, the molecular connectivity of *P. hirondellei* has been established in the Cantabrian Sea using ddRADseq-derived SNPs, but within a limited geographic range (Busch et al., 2020). Here, our aim was to provide a phylogenetic framework for our specimens, in order to properly delimit these *Phakellia* species (Pante et al., 2015), which can be challenging to identify. For *P. robusta* we also investigated the genetic diversity, molecular connectivity, and microbial community structure over a wide geographic (10s–1000 s km) and bathymetric (29–1,150 m) range. In addition, we studied the potential introgression patterns (*i.e.* exchange of genes between genetically differentiated species) between the two *Phakellia* species. To achieve that, we used different sources of evidence such as traditional markers, ddRADseq-derived SNPs, and *16S* amplicon sequencing of the microbial communities. We included sampling sites from three Marine Protected Areas: (1) the Hatton-Rockall Basin MPA (UK), designated in 2014 (https://jncc.gov.uk/our-work/hatton-rockall-basin-mpa/); (2) the Sula Ridge, comprising the Sula Reef (Norway); and (3) *El Cachucho* (Cantabrian Sea) MPA, designated in 2008 (Heredia et al., 2008). In particular, the occurrence and distribution of *P. robusta*, among other species, in this area has been a key element in the design of the Master Management Plan for this MPA (Rodríguez-Basalo et al., 2019). We also included areas with different levels of protection including: the Avilés Canyon System in the Cantabrian Sea, established as Site of Community Importance in 2015; and the Kerry Heads, designated as a Special Area of Conservation by Ireland in 2016.

2. Material and methods

2.1. Sample collection and preservation

A total of 46 specimens of fan-shaped sponges of *Phakellia robusta* (n=23) and *Phakellia hirondellei* (n=23) were collected from seven different sites (Avilés Canyon System, *El Cachucho* MPA, Hatton-Rockall Basin, Kerry Head Reefs, NW of Orkney, Korsfjorden, and Sula Reef in the NE Atlantic; Fig. 1, Table 1). Samples from the Cantabrian Sea (including samples from Avilés Canyon System and *El Cachucho* MPA)

were collected using a rock dredge during the SponGES0617 cruise on board the Spanish *R/V Ángeles Alvariño*, June 2017. Samples from Korsfjorden were collected using a triangular dredge on board the *R/V Hans Brattstrøm*, in September 2016, while the only sample from the Sula Reef was collected using the ROV ÆGIR 6000 on board the *R/V G.O. Sars*, July 2017. Samples from Kerry Head Reefs were collected using an anchor dredge on board the *R/V Celtic Voyager*, August 2013. Samples from Hatton-Rockall Basin where collected by Agassiz trawl on board the *MFV Scotia*, July 2015. Samples from NW of Orkney were collected from a commercial fishing vessel, May 2018. In addition, we collected other fan-shaped sponges for the phylogenetic reconstruction and the microbial analysis: *Phakellia ventilabrum* (Linnaeus, 1767) (n=15), *Phakellia rugosa* (Bowerbank, 1866) (n=4), and *Axinella infundibuliformis* (Linnaeus, 1759) (n=3), and Axinellidae sp. (n=1), including samples from the Cantabrian Sea, the Kerry Head Reefs, the Rockall Plateau, Norway, and the Barents Sea (Table 1).

Upon collection, all sponges were cleaned with fresh seawater to remove the mud and photographed alive. Sponge fragments (ranging 1–3 cm^3) of each specimen were cut and preserved in 96% EtOH for molecular analysis (see below), and immediately stored at −20 °C; EtOH was replaced three times after one day preservation. A small portion of all specimens was also incubated in bleach and kept at room temperature for several days for spicule analysis (see below).

Samples were used for different purposes, including barcoding, phylogenetic analysis, ddRADseq, and microbial characterization (see Table 1).

2.2. Morphological analysis

For the study of dissociated spicules, the organic matter was digested in sodium hypochlorite and then washed three times, first with water, second with 50% EtOH and finally with 96% EtOH. A few drops of spicule solution were then placed on a stub, which was coated with gold using a 208HR Cressington Sputter Coater, and examined with a Zeiss Gemini Ultra plus SEM at the Natural History Museum of London. Spicule measurements were made in an Olympus BX43 compound microscope (Olympus Corporation, Japan) with an Olympus UC50 camera and cellSens Standard interface v.1.16 (Olympus Corporation, Japan). Data for spicule sizes was based on 20 measurements for each spicule category, comprising minimum, average, and maximum lengths in

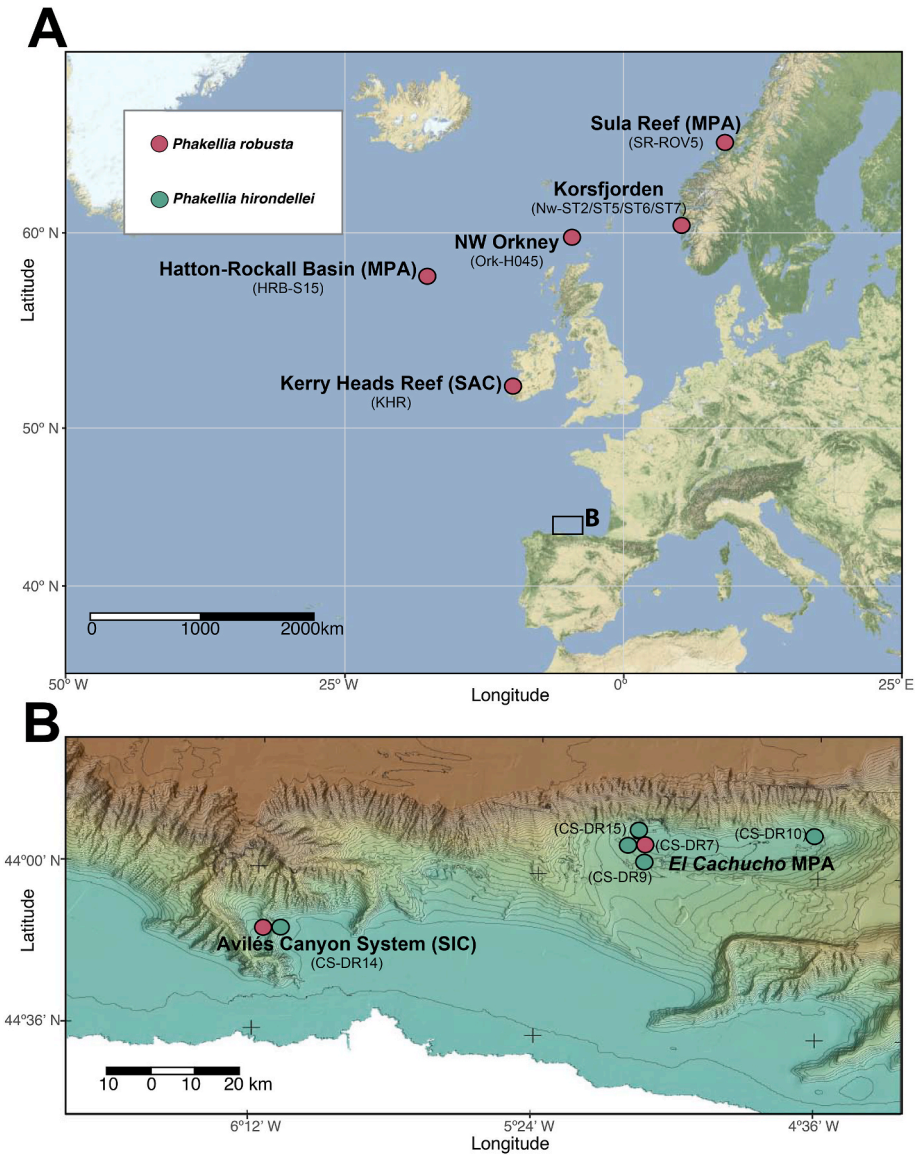

Fig. 1. A. Map of the study area including the information on the areas (in bold) and sampling sites (in brackets) where samples of *Phakellia* species were collected. **B.** Map of the Cantabrian Sea identifying the areas (in bold) and sampling sites (in brackets).

Table 1
List of specimens used in the study grouped by taxon. Region, area, coordinates and depth are provided. The type of information generated for each specimen is also indicated. †*MPA* Marine Protected Area, *SAC* Special Area of Conservation, *SCI* Site of Community Importance.

Taxon/Specimen code	Sampling station	Region	Area	Degree conservation†	Latitude	Longitude	Depth (m)	*COI*	ddRAD	Microbial analysis
Phakellia hirondellei										
Phiron-CS-DR14-652	CS-DR14	Cantabrian Sea	Avilés Canyon System	SCI	43°52.080′N	6°08.549′W	340	Yes	Yes	Yes
Phiron-CS-DR15-851b	CS-DR15	Cantabrian Sea	*El Cachucho*	MPA	44°06.344′N	5°09.027′W	650	–	Yes	Yes
Phiron-CS-DR15-856	CS-DR15	Cantabrian Sea	*El Cachucho*	MPA	44°06.344′N	5°09.027′W	650	–	Yes	Yes
Phiron-CS-DR15-857b	CS-DR15	Cantabrian Sea	*El Cachucho*	MPA	44°06.344′N	5°09.027′W	650	Yes	Yes	Yes
Phiron-CS-DR15-857c	CS-DR15	Cantabrian Sea	*El Cachucho*	MPA	44°06.344′N	5°09.027′W	650	Yes	Yes	Yes
Phiron-CS-DR15-857d	CS-DR15	Cantabrian Sea	*El Cachucho*	MPA	44°06.344′N	5°09.027′W	650	Yes	–	–
Phiron-CS-DR15-857e	CS-DR15	Cantabrian Sea	*El Cachucho*	MPA	44°06.344′N	5°09.027′W	650	Yes	Yes	Yes
Phiron-CS-DR15-869b	CS-DR15	Cantabrian Sea	*El Cachucho*	MPA	44°06.344′N	5°09.027′W	650	–	Yes	Yes
Phiron-CS-DR15-976	CS-DR15	Cantabrian Sea	*El Cachucho*	MPA	44°06.344′N	5°09.027′W	650	Yes	Yes	Yes
Phiron-CS-DR7-251	CS-DR7	Cantabrian Sea	*El Cachucho*	MPA	44°06.2027′N	5° 09.0580′W	660	Yes	Yes	Yes
Phiron-CS-DR7-253	CS-DR7	Cantabrian Sea	*El Cachucho*	MPA	44°06.2027′N	5° 09.0580′W	660	Yes	Yes	Yes
Phiron-CS-DR9-380	CS-DR7	Cantabrian Sea	*El Cachucho*	MPA	44°06.2027′N	5° 09.0580′W	660	Yes	Yes	Yes
Phiron-CS-DR9-383	CS-DR7	Cantabrian Sea	*El Cachucho*	MPA	44°06.2027′N	5° 09.0580′W	660	Yes	Yes	Yes
Phiron-CS-DR9-400	CS-DR7	Cantabrian Sea	*El Cachucho*	MPA	44°06.2027′N	5° 09.0580′W	660	Yes	–	–
Phiron-CS-DR10-455	CS-DR10	Cantabrian Sea	*El Cachucho*	MPA	44°06.080′N	4°38.300′W	541	Yes	Yes	Yes
Phiron-CS-DR10-456	CS-DR10	Cantabrian Sea	*El Cachucho*	MPA	44°06.080′N	4°38.300′W	541	Yes	Yes	Yes
Phiron-CS-DR10-457	CS-DR10	Cantabrian Sea	*El Cachucho*	MPA	44°06.080′N	4°38.300′W	541	Yes	Yes	Yes
Phiron-CS-DR10-458	CS-DR10	Cantabrian Sea	*El Cachucho*	MPA	44°06.080′N	4°38.300′W	541	Yes	Yes	Yes
Phiron-CS-DR10-459	CS-DR10	Cantabrian Sea	*El Cachucho*	MPA	44°06.080′N	4°38.300′W	541	Yes	Yes	Yes
Phiron-CS-DR10-464	CS-DR10	Cantabrian Sea	*El Cachucho*	MPA	44°06.080′N	4°38.300′W	541	Yes	Yes	Yes
Phiron-CS-DR10-465	CS-DR10	Cantabrian Sea	*El Cachucho*	MPA	44°06.080′N	4°38.300′W	541	Yes	Yes	Yes
Phiron-CS-DR10-466	CS-DR10	Cantabrian Sea	*El Cachucho*	MPA	44°06.080′N	4°38.300′W	541	Yes	Yes	Yes
Phiron-CS-DR10-468	CS-DR10	Cantabrian Sea	*El Cachucho*	MPA	44°06.080′N	4°38.300′W	541	Yes	Yes	Yes
Phiron-CS-DR10-470	CS-DR10	Cantabrian Sea	*El Cachucho*	MPA	44°06.080′N	4°38.300′W	541	Yes	Yes	Yes
Phiron-CS-DR10-498	CS-DR10	Cantabrian Sea	*El Cachucho*	MPA	44°06.080′N	4°38.300′W	541	Yes	Yes	Yes
Phakellia robusta										
Prob-CS-DR7-244	CS-DR7	Cantabrian Sea	*El Cachucho*	MPA	44°06.2027′N	5° 09.0580′W	660	Yes	Yes	Yes
Prob-CS-DR14-651	CS-DR14	Cantabrian Sea	Avilés Canyon System	SCI	43°52.080′N	6°08.549′W	340	Yes	Yes	Yes
Prob-CS-DR14-653	CS-DR14	Cantabrian Sea	Avilés Canyon System	SCI	43°52.080′N	6°08.549′W	340	Yes	Yes	Yes
Prob-KHR-13	KHR	Kerry Head Reefs, SW Ireland	Kerry Head Reefs	SAC	52° 20.5824′N	10° 44.1023′W	105	Yes	Yes	Yes
Prob-KHR-21	KHR	Kerry Head Reefs, SW Ireland	Kerry Head Reefs	SAC	52° 20.5824′N	10° 44.1023′W	105	Yes	Yes	Yes
Prob-HRB-S15-13	HRB-S15	Rockall Plateau	Hatton-Rockall Basin	MPA	58°05.86020′N	16°16.00980′W	1150	Yes	Yes	Yes
Prob-HRB-S15-13-1-2	HRB-S15	Rockall Plateau	Hatton-Rockall Basin	MPA	58°05.86020′N	16°16.00980′W	1150	Yes	Yes	Yes
Prob-HRB-S15-13-2-2	HRB-S15	Rockall Plateau	Hatton-Rockall Basin	MPA	58°05.86020′N	16°16.00980′W	1150	Yes	Yes	Yes
Prob-Ork-H045-01803	Ork-H045	NW of Orkney	NW of Orkney	–	60°01.05000′N	4°07.71000′W	132–145	Yes	Yes	Yes
Prob-Nw-ST2-28	Nw-ST2	Norway	Korsfjorden	–	59° 58.8790′N	5° 22.4371′E	97–332	Yes	Yes	Yes
Prob-Nw-ST2-29	Nw-ST2	Norway	Korsfjorden	–	59° 58.8790′N	5° 22.4371′E	97–332	Yes	Yes	Yes
Prob-Nw-ST2-30	Nw-ST2	Norway	Korsfjorden	–	59° 58.8790′N	5° 22.4371′E	97–332	Yes	Yes	Yes
Prob-Nw-ST5-37	Nw-ST5	Norway	Korsfjorden	–	59° 48.8155′N	5° 36.2325′E	226–292	Yes	Yes	Yes
Prob-Nw-ST5-48	Nw-ST5	Norway	Korsfjorden	–	59° 48.8155′N	5° 36.2325′E	226–292	–	Yes	Yes
Prob-Nw-ST6-62	Nw-ST6	Norway	Korsfjorden	–	59° 52.3700′N	5° 32.9939′E	29–213	Yes	Yes	Yes
Prob-Nw-ST6-63	Nw-ST6	Norway	Korsfjorden	–	59° 52.3700′N	5° 32.9939′E	29–213	Yes	Yes	Yes
Prob-Nw-ST6-64	Nw-ST6	Norway	Korsfjorden	–	59° 52.3700′N	5° 32.9939′E	29–213	Yes	Yes	Yes
Prob-Nw-ST6-65	Nw-ST6	Norway	Korsfjorden	–	59° 52.3700′N	5° 32.9939′E	29–213	Yes	Yes	Yes
Prob-Nw-ST6-66	Nw-ST6	Norway	Korsfjorden	–	59° 52.3700′N	5° 32.9939′E	29–213	Yes	Yes	Yes
Prob-Nw-ST6-A	Nw-ST6	Norway	Korsfjorden	–	59° 52.3700′N	5° 32.9939′E	29–213	Yes	Yes	Yes
Prob-Nw-ST6-B	Nw-ST6	Norway	Korsfjorden	–	59° 52.3700′N	5° 32.9939′E	29–213	Yes	Yes	Yes
Prob-Nw-ST7-78	Nw-ST7	Norway	Korsfjorden	–	59° 52.4985′N	5° 32.8076′E	95–253	Yes	Yes	Yes
Prob-SR-ROV5-13	SR-ROV5	Sula Ridge, Norway	Sula Reef	MPA	64° 4.488′N	8° 1.626′E	295	Yes	Yes	Yes
Phakellia ventilabrum										
Pven-CS-DR14-650	CS-DR14	Cantabrian Sea	Avilés Canyon System	SCI	43°52.080′N	6°08.549′W	340	Yes	–	Yes
Pven-CS-DR1-02	CS-DR1	Cantabrian Sea	*El Cachucho*	MPA	43° 43.703′N	5° 50.480′W	240	Yes	–	–
Pven-KHR-Ev51A	KHR	Kerry Head Reefs, SW Ireland	Kerry Head Reefs	SAC	52° 20.5824′N	10° 44.1023′W	105	Yes	–	–

(*continued on next page*)

Table 1 (*continued*)

Taxon/Specimen code	Sampling station	Region	Area	Degree conservation†	Latitude	Longitude	Depth (m)	*COI*	ddRAD	Microbial analysis
Pven-RB-H027-01408	RB-H027	Rockall Plateau	Rockall Bank	–	57° 25.140′N	13° 27.600′W	181	Yes	–	–
Pven-RB-H028-01627	RB-H028	Rockall Plateau	Rockall Bank	–	57° 38.880′N	12° 59.760′W	303	Yes	–	–
Pven-Nw-SPX-22	Nw-ST2	Norway	Korsfjorden	–	59° 58.8790′N	5° 22.4371′E	97–332	Yes	–	–
Pven-Nw-ST2-23	Nw-ST2	Norway	Korsfjorden	–	59° 58.8790′N	5° 22.4371′E	97–332	Yes	–	–
Pven-Nw-SPX-24	Nw-ST2	Norway	Korsfjorden	–	59° 58.8790′N	5° 22.4371′E	97–332	Yes	–	–
Pven-Nw-SPX-30	Nw-ST5	Norway	Korsfjorden	–	59° 48.8155′N	5° 36.2325′E	226–292	Yes	–	–
Pven-Nw-SPX-31	Nw-ST5	Norway	Korsfjorden	–	59° 48.8155′N	5° 36.2325′E	226–292	Yes	–	–
Pven-Nw-SPX-99	KB63	W Norway	Shelf	–	60° 37.68′N	4° 39.8554′E	239–257	Yes	–	–
Pven-Nw-SPX-123	KB32	W Norway	Shelf	–	59° 52.7970′N	4° 42.3118′E	224–230	Yes	–	–
Pven-BS-31	GS2017110-68	W Barents Sea	Tromsøflaket	–	71° 23.7104′N	16° 48.9593′E	330	Yes	–	–
Pven-BS-32	GS2017110-68	W Barents Sea	Tromsøflaket	–	71° 23.7104′N	16° 48.9593′E	330	Yes	–	–
Pven-BS-33	GS2017110-68	W Barents Sea	Tromsøflaket	–	71° 23.7104′N	16° 48.9593′E	330	Yes	–	–
Phakellia rugosa										
Prug-Nw-ST5-41	Nw-ST5	Norway	Korsfjorden	–	59° 48.8155′N	5° 36.2325′E	226–292	–	Yes	Yes
Prug-Nw-SPX-40	Nw-ST2	Norway	Korsfjorden	–	59° 58.8790′N	5° 22.4371′E	97–332	Yes	–	–
Prug-Nw-SPX-43	Nw-ST5	Norway	Korsfjorden	–	59° 48.8155′N	5° 36.2325′E	226–292	Yes	–	–
Prug-Nw-SPX-137	ESP-2016-1	W Norway	Scorpo, Korsfjorden	–	60° 15.3533′N	5° 17.5067′E	230–400	Yes	–	–
Axinella infundibuliformis										
Ainf-Nw-SPX-28	Nw-ST5	Norway	Korsfjorden	–	59° 48.8155′N	5° 36.2325′E	226–292	Yes	–	–
Ainf-Nw-SPX-29	Nw-ST5	Norway	Korsfjorden	–	59° 48.8155′N	5° 36.2325′E	226–292	Yes	–	–
Ainf-Nw-ST5-45	Nw-ST5	Norway	Korsfjorden	–	59° 48.8155′N	5° 36.2325′E	226–292	–	–	Yes
Axinellidae sp.										
Axin-RB-H025-01411	RB-H025	Rockall Plateau	Rockall Bank	–	57°10.23′N	13°38.28′W	185–189	–	–	Yes

micrometers (μm).

2.3. DNA extraction, amplification, and sequencing of COI

DNA was extracted from all samples using the DNeasy Blood & Tissue kit (Qiagen, www.qiagen.com) following the manufacturer's protocol, except for the cell lysis time which was conducted overnight and the final DNA elution step, performed twice using 75 μL of elution buffer in order to increase DNA concentration. Double-stranded DNA was quantified with Qubit dsDNA HS assay (Life Technologies).

We amplified a fragment of the mitochondrial cytochrome *c* oxidase subunit I (*COI*) using the primers HCO1490 and LCO2198 (Folmer et al., 1994), but those produced clean chromatograms only for the specimens identified as *P. ventilabrum*, *P. rugosa*, and *A. infundibuliformis*. To obtain clean sequences for *P. robusta* and *P. hirondellei* we designed specific primers based on the *COI* sequence retrieved from their transcriptomes (Cranston et al., 2021): (i) the primers Pcant-COIF (5′-TTTGCAGGGA TGATCGGAAC-3′) and Pcant-COIR (5′-CCCGGGGCCCTCATATTTAA-3′) to amplify *P. hirondellei* samples; and (ii) the primers Prob -COIF5′-GCGGGTATGATAGGAACAGC-3′) and Prob-COIR (5′-ACCCGG CGCTCTCATATTTA3′) to amplify the samples of *P. robusta*. The primers for *P. robusta* were designed to amplify a region with introns present in some specimens. PCR program for all *COI* markers was 94 °C/5 min – (94 °C/30 s–58 °C/30 s–72 °C/30 s) x 35 cycles – 72 °C/10 min.

All DNA markers were amplified in 12.5 μL reactions using 10.5 μL of VWR REDTaq® DNA Polymerase 1.1x Master Mix (VWR, USA), 0.5 μL of the forward and reverse primers, and 1 μL of DNA template. PCR products, stained with GelRed® (Biotium, USA), were visualized in a 2.5% agarose gel electrophoresis, run at 90 V for 30 min. Sequencing was conducted on an ABI 3730XL DNA Analyser (Applied Biosystems, USA) at the Molecular Core Labs (Sequencing Facility) of the Natural History Museum of London (NHM), using the forward and reverse primers mentioned above. Successfully amplified and sequenced specimens are indicated in Table 1.

2.4. Phylogenetic and haplotype network analyses

Overlapping *COI* sequence fragments were assembled and trimmed into consensus sequences using the software *Geneious* v.10.1.3 (http://www.geneious.com, Kearse et al., 2012). Occasionally, only forward or reverse sequences were used due to the poor quality of one of the fragments. Consensus sequences were checked for contamination using BLAST (Altschul et al., 1990), and aligned with the inbuilt MAFFT v.7.309 (Katoh and Standley, 2013), using the Q-INS-I option.

Our *COI* alignment (406 bp) consisted of 64 newly generated sequences and a selection of 20 sponge species whose sequences were available from NCBI (accession numbers on Fig. 2 and Suppl. Table 1). For some *P. robusta* specimens, an intronic region was removed from the sequences before conducting the alignment (Cranston et al., 2021). Nucleotide substitution models were fitted using *jModelTest* v.2.1.7 (Darriba et al., 2012), with the number of substitution schemes set to three. Based on the Akaike Information Criterion (AIC) (Akaike, 1998), the best fit model was GTR+I+G. Maximum Likelihood (ML) analyses were implemented using *RAxML* v.8.2.10 (Stamatakis, 2014), using GTR+I+G as model, partitioned into codon positions, with 10 runs and 100 bootstrap replicates. The resulting tree was visualized and edited in FigTree v.1.4.2 (Rambaut, 2014).

The *COI* alignment was used to build haplotype networks for the different *Phakellia* species separately in *PopART* v. 1.7 (Leigh and Bryant, 2015) using the TCS network algorithm (Clement et al., 2000). Minimum genetic distances based on uncorrected *p*-distance and Kimura two-parameter (K2P) models between and within *Phakellia* species were calculated with the program *MEGA* v. 7.0.26 (Kumar et al., 2018).

2.5. ddRADseq library preparation and sequencing

ddRADseq libraries were performed for a total of 46 individuals from two different species, *P. robusta* (n = 23) and *P. hirondellei* (n = 23) (see Table 1). Ten out of the 23 individuals of *P. hirondellei* were already used in a paper by Busch et al. (2020). Library preparation was conducted following Peterson et al. (2012) with some modifications following also Combosch et al. (2017). Double-stranded genomic DNA (500 ng) was digested using the high-fidelity restriction enzymes SbfI and EcoRI (New England Biolabs) for 6 h at 37 °C. Resulting digested fragments were cleaned by manual pipetting using Agencourt AMPure beads (1.5X volume ratio; Beckham Coulter), and were subsequently quantified with a Qubit dsDNA HS assay (Life Technologies). Resulting fragments were ligated to custom-made P1 and P2 adapters containing sample-specific barcodes and primer annealing sites. Barcoded individuals were pooled into libraries, cleaned by manual pipetting using AMPure beads (1.5X volume ratio), and size-selected (range sizes 200–400 bp) using a BluePippin (Sage Science). Each library was PCR-amplified with Phusion polymerase (Thermo Scientific) and using a different set of PCR primers to allow for multiplexing libraries. The PCR program used was 98 °C/30 s – (98 °C/10 s–65 °C/30 s–72 °C/1.5 min) x 12 cycles – 72 °C/10 min. Resulting PCR products were cleaned by manual pipetting using Agencourt AMPure beads (1.5X volume ratio), quantified with a Qubit dsDNA HS assay, and quality-checked on a Tapestation 2200 (Agilent Technologies). Libraries were pooled normalizing their concentration, and pooled together with RNA-seq libraries in the same flow cell. Libraries pair-end sequenced (150 bp) were run on an Illumina HiSeq4000 (Illumina) at Macrogen Inc. (South Korea).

2.6. ddRADseq locus assembly, filtering and outlier detection

Quality filtering and locus assembly was conducted with the *Stacks* pipeline v. 2.41 (Catchen et al., 2013). RAD-tags (DNA fragments with the two appropriate restriction enzyme cut sites that were selected, amplified, and sequenced) were processed using *process_radtags*, where low quality raw reads were trimmed, as well as reads with uncalled bases, and reads without a complete barcode or restriction cut site. The *process_radtags* rescue feature (*-r*) was used to recover minimally diverged barcodes and RAD-tags (*–barcode_dist 3*; *–adapter_mm 2*). The *process_radtags* trimming feature (*-t*) was used to trim remaining reads to 120 bp, in order to increase confidence in SNP calling. After performing these filtering steps, we retained a total of 254,152,192 reads from the initial 332,139,090 raw reads (76.5% of reads were retained), with an average of 3,099,417 reads per sample.

We conducted optimization tests following Jeffries et al. (2016) and Paris et al. (2017) for the parameters *m*, *M*, and *n* in our dataset. Briefly, tests were carried out for five sets of three randomly chosen individuals and, for each test, all non-test parameters were kept as default. The *Stacks populations* module was run to filter data with r = 0.8 for each test, and the number of assembled loci, number of polymorphic loci, number of SNPs, and coverage was compared between the tests. Final parameter values were as follows: *ustacks*: M=2, m=3; *cstacks*: n=3. The subsequent run of the *Stacks* pipeline (*ustacks*, *cstacks*, *sstacks*, *tsv2bam*, and *gstacks*) using the 46 individuals recovered a mean locus coverage among all samples of 47.1±13.0, ranging from 15.8 to 99.5.

The *Stacks populations* module was used to obtain two datasets: *P. robusta* and the combined dataset of *P. robusta-P. hirondellei*. This module was used to conduct a first filtering of the data, retaining those SNPs present in at least 70% of the individuals (r = 0.7), and just retaining the first SNP from each RAD-tag using *–write_single_SNP*, in order to reduce the linkage disequilibrium among loci. In order to diminish errors in the estimation of SNPs showing signatures of selection (Roesti et al., 2012), we only retained SNPs with a minimum allele frequency (*–min_maf*) > 0.05. Also, SNPs departing from Hardy-Weinberg equilibrium (*p*-value = 0.05) and SNPs showing an excess of heterozygosity ($H_o > 0.5$) (Hohenlohe et al., 2011) were also removed. Given the known presence of symbiotic bacteria in the tissue *Phakellia* species, the resulting set of sequences containing variable SNPs obtained after running *Stacks populations* were filtered for bacterial hits. This was done using *–blastn* comparing the above mentioned set of sequences against a nr database extracted from NCBI (accessioned on October 21, 2019), using a e-value of 1e-6 or lower. This filtering for bacteria resulted in 1 hit for the *P. robusta* dataset and 0 hits for the *P. robusta-P. hirondellei* dataset.

Additional filtering was performed using the *adegenet* R package (Jombart 2008; Jombart & Ahmed 2011; Team, 2017), to more accurately assess SNP distributions across individual samples and sampling stations, and to test different filtering thresholds to maximise the number of retained SNPs and minimise missing data. This approach provides significant insight for defining final thresholds in comparison with the *Stacks populations* module. This was combined with the visualization of the data using the Matrix Condenser interface (https://bmedeiros.shinyapps.io/matrix_condenser/; de Medeiros and Farrell, 2018). The threshold exploration resulted in no more filtering of samples or SNPs.

In order to differentiate neutral SNPs from putative SNPs under selection, the dataset of *P. robusta* was analysed using two different programs *ARLEQUIN* v. 3.5 (Excoffier and Lischer, 2010) and *BAYESCAN* v. 2.1 (Foll & Gaggioti, 2008). For the *ARLEQUIN* analysis, we set the 'Allowed missing level per site' to 0.05 and used the 'Non-hierarchical island model'; *p*-values obtained were corrected using the *p.adjust* function in R with the *fdr* method, corresponding to the 'BH' in Benjamini and Hochberg (1995). *BAYESCAN* was run with default parameters and considered outlier SNPs those with a *q*-value < 0.05, which is the FDR analogue of the *p*-value. For the *P. robusta* dataset, *ARLEQUIN* and *BAYESCAN* returned a total of 50 and 0 SNPs under selection respectively. These 50 SNPs were removed for subsequent analyses, which resulted in a final dataset of 428 SNPs for *P. robusta*. The combined *P. robusta-P. hirondellei* dataset had 376 SNPs.

2.7. Population genomic analyses

We calculated genetic diversity and demographic statistics for *P. robusta* with the SNP dataset. We grouped the samples per sampling station and also by region: a total of four regions were considered including the Cantabrian Sea, Kerry Head Reefs, Hatton-Rockall Basin, and Orkney-Norway, the latter region considering together samples collected from Korsfjorden, Sula Reef, and NW of Orkney (see Table 1). Expected (*He*) and observed (*Ho*) heterozygosity and inbreeding coefficients (F_{IS}) were calculated per region and for the whole dataset using *Genodive* v. 3.02 (Meirmans and Van Tienderen, 2004).

We assessed the population structure for *P. robusta* using two different methods: *STRUCTURE* v. 2.3 (Pritchard et al., 2000), and the discriminant analysis of principal components (*DAPC*) as implemented in the *adegenet* R package (Jombart et al., 2010). We ran *STRUCTURE* with 200,000 MCMC iterations using the admixture model, with a burn-in of 100,000 iterations, setting the putative *K* from 1 to 10 with 15 replicates for each run. We used *STRUCTURE HARVESTER* (Earl and vonHoldt, 2012) and *CLUMPP* v. 1.1.2 (Jakobsson and Rosenberg, 2007) to determine the most likely number of clusters and to average each individual's membership coefficient across the *K* value replicates, respectively. Population structure in *DAPC* was assessed with the function *snapclust* using the genetic clustering mode *snapclust.choose.k*. This was done using the Bayesian Information Criterion (BIC) function using the k-means algorithm (*pop.ini = "kmeans"*), allowing a maximum K (*number of clusters*) of 6 (max = *6*), and a maximum number of iterations of 100 (*max.iter = 100*). To identify the optimal number of clusters, k-means is run sequentially with increasing values of k, and different clustering solutions are compared using Bayesian Information Criterion (BIC), being the optimal clustering solution the one that corresponds to the lowest BIC number. After defining the optimal number of clusters for each dataset, the number of retained principal components (PCs) axes and eigen values were chosen using the cross-validation *xvalDapc*

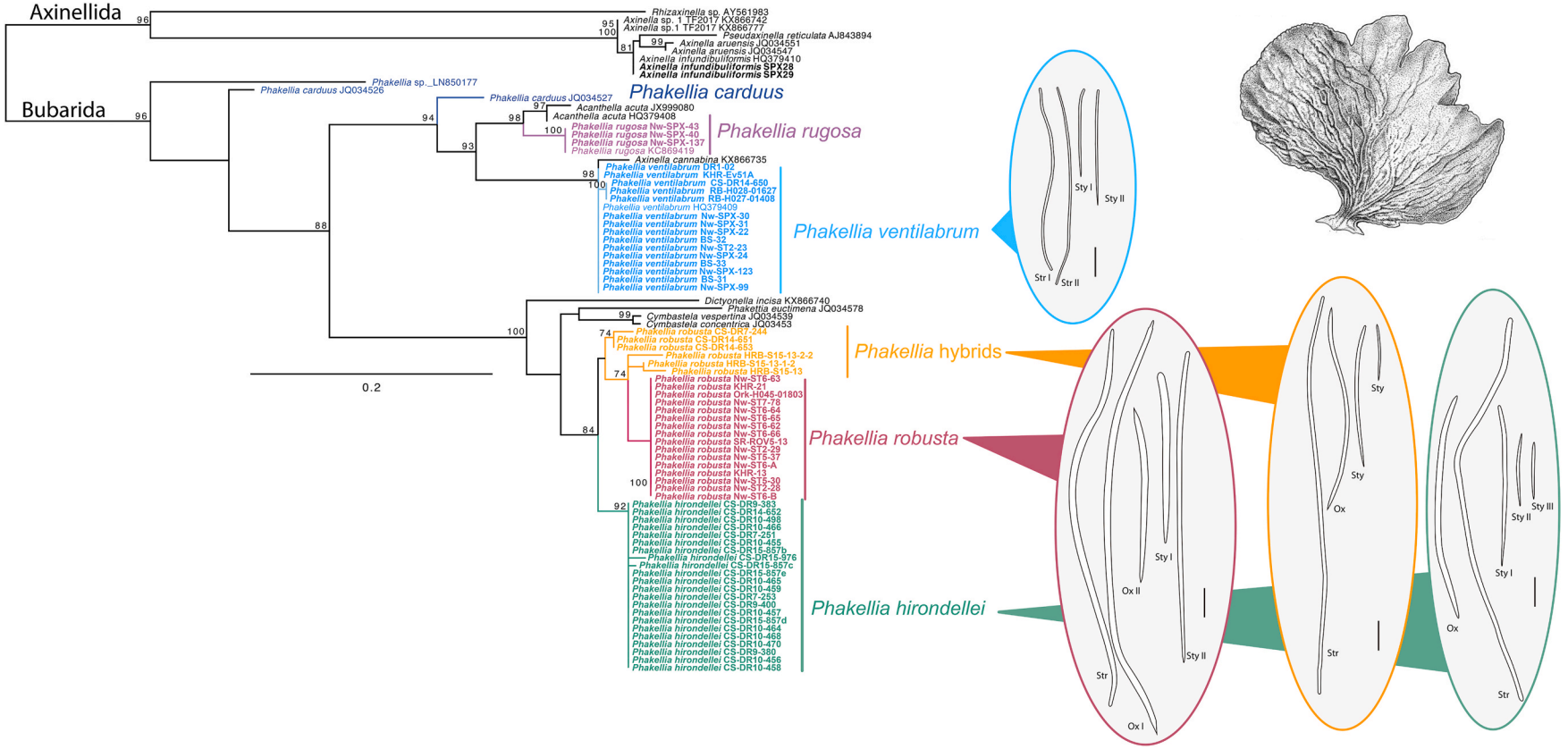

Fig. 2. *COI* phylogenetic tree of a selection of demosponges using Maximum likelihood (ML). *Phakellia ventilabrum*, *P. robusta* and *P. hirondellei* are identified with different colours. Only bootstrap values > 75 are reported. Specimens sequenced here are in bold. Schematics of the different types of megascleres present in *P. ventilabrum*, *P. robusta*, *P. hirondellei* and the hybrids of *P. robusta* are depicted. *Ox* oxea, *Str* strongyle, *Sty* style. External appearance of a fan-shape *Phakellia*-like specimen is also depicted. (For interpretation of the references to colour in this figure legend, the reader is referred to the Web version of this article.)

function from the *adegenet* R package with a number of replicates of 1,000 (*n.rep = 1000*). *xvalDapc* provides an objective optimization procedure for identifying the lowest number of PCs retaining the maximum variance, which is associated with the lowest mean squared error (*MSE*). The *DAPC* function *assignplot* was used to plot the probabilities of assignment of the different individuals to the different clusters, while the function *scatter.plot* was used to produce scatterplots of PCs with eigen values as inset.

In addition, a hierarchical analysis of molecular variance (*AMOVA*) was performed for the *P. robusta* dataset using *ARLEQUIN*, to test whether the geographical grouping that resulted from the structuring analyses explained a significant part of the total genetic variation. *AMOVA* was performed with samples being grouped into four regions (Cantabrian Sea, Kerry Head Reefs, Hatton-Rockall Basin, and Orkney-Norway, the latter including Korsfjorden, Sula Reef, and NW of Orkney) and also by grouping samples by depth ranges (Shallow: including Kerry Head Reefs, Korsfjorden, Sula Reef, and NW of Orkney; Deep: including Cantabrian Sea and Hatton-Rockall Basin).

Pairwise F_{ST} values for the *P. robusta* dataset was estimated to measure the differentiation between the four regions mentioned above using *ARLEQUIN*, using the default parameters with 10,000 permutations. *Barrier* v. 2.2 (Manni et al., 2004) was then used to identify and locate genetic breaks for *P. robusta*. Finally, in order to identify current gene flow patterns in *P. robusta* in the study area, Nei's G_{ST} method with 1,000 bootstrap was used to estimate the relative contemporary asymmetric migration between regions, using the *divMigrate* function of the *diveRsity* R package (Sundqvist et al., 2016).

2.8. Detection of hybridization

The combined dataset of *P. robusta-P. hirondellei* was analysed together using a similar approach as the one described above (by running *STRUCTURE* and *DAPC*) to investigate the current pattern of genetic structure and interspecific introgression. We also used the hierarchical clustering function *hclust* in R to perform a Ward clustering on the allele data using the *ward.D2* method (Müllner, 2013). Since we observed discordant signals in the assignment of samples to the two different species and signatures of introgression between the two species (see Results section below), we decided to further investigate for possible hybridization signatures. Using the combined dataset of *P. robusta-P. hirondellei* we run the function *hybridize* in *adegenet* to simulate a population of 50 hybrid individuals between the two species, and subsequently analysed the structure of both real and simulated individuals together using the same pipeline described above (*snapclust.choose.k*, *snapclust*, *xvalDapc*, and *dapc* functions). Alternatively, we used the *fineRADstructure* package (Malinsky et al., 2018) to assess the shared ancestry in the *P. robusta-P. hirondellei* dataset. This package uses ddRAD-haplotype linkage information and gets high-resolution co-ancestry data. The file used in this analysis was obtained after running *populations* on the set of 376 SNPs *P. robusta-P. hirondellei* deselecting the *–write_single_SNP* option, thus allowing for linked SNPs in the different RAD-tags, resulting in a final dataset of 2,775 SNPs. *fineRADstructure* was run with the default values following the indications at the online tutorial (http://cichlid.gurdon.cam.ac.uk/fineRADstructure.html): x 100,000, -y 100,000, -z 1,000 to assign individuals to populations, and -x 10,000 for the tree building. Graphic interpretation of the results was performed using Finestructure R Library and *fineRADstructurePlot.R* script, both provided in the *fineRADstructure* package.

Finally, genetic diversity and demographic statistics were calculated separately for *P. robusta* and *P. hirondellei* with the SNP datasets using *Genodive*. In this case we distinguished between hybrids and non-hybrids.

2.9. Microbial analyses: 16S amplicon sequencing

We analysed the microbial community composition of all the specimens of *P. robusta* and *P. hirondellei* used in the ddRADseq analyses (Table 1). Apart from these organisms, we also analysed the microbial community composition of one specimen of *P. ventilabrum* from the Cantabrian Sea (Pven-CS-DR14-650), one specimen of *Axinella infundibuliformis* (Ainf-Nw-ST5-45) and one specimen of *Phakellia rugosa* (Prug-Nw-ST5-41) from Norway, and one specimen of Axinellidae sp. from the Rockall Bank (Axin-RB-H025-01411).

Samples for microbial analyses were flash-frozen on board the research vessel and stored at −80 °C. DNA extraction was done with ca. 0.25 g of sponge tissue, using the DNeasy Power Soil kit (Qiagen, Venlo, Netherlands), and quality and quantity of the DNA extracts was assessed using a NanoDrop spectrophotometer. We targeted the V3–V4 variable regions of the *16S* gene using the primer pair 341F-806R (Muyzer et al., 1993; Caporaso et al., 2011) in a one-step PCR (98 °C 30s, 30x [98 °C 9s, 55 °C 60s, 72 °C 90s] 72 °C 10min) with a dual barcoding approach (Kozich et al., 2013). After quality assessment of the PCR products (gel electrophoresis), samples were normalised (SequalPrep Normalization Plate Kit; Thermo Fisher Scientific, Waltham, USA) and pooled. Using v3 chemistry, sequencing was performed on a MiSeq platform (MiSeqFGx, Illumina, San Diego, USA).

For the demultiplexing step, zero mismatches were allowed in the barcode sequence. We processed raw reads within the *QIIME2* v. 2018.11 environment (Bolyen et al., 2018). The *DADA2* algorithm (Callahan et al., 2016) was applied on forward reads (truncated to 270 nt) to generate Amplicon Sequence Variants (ASVs). Calculation of phylogenetic trees was performed on the produced ASVs, using the *FastTree2* plugin within *QIIME2*. We trained a primer-specific Naïve Bayes taxonomic classifier based on the Silva 132 99% OTUs *16S* database (Quast et al., 2013) and used this classifier for taxonomic classification of representative ASVs. Weighted UniFrac distances (phylogeny-based beta diversity) were calculated (Lozupone and Knight, 2005) and used as the basis for computing a clustering dendrogram in *QIIME2* and *ITOL* (Letunic and Bork, 2016). Based on the clustering dendrogram, we examined which sponge individuals belonged to the same microbial cluster. To determine whether microbial phyla differed significantly across sponge microbial cluster, we used the Linear Discriminant Analysis (LDA) Effect Size (*LEfSe*) algorithm (Segata et al., 2011). Based on this algorithm, microbial phyla which differed across sponge microbial clusters were ranked according to the estimated effect sizes. For the microbial phyla turning out as significantly enriched in a particular sponge microbial cluster based on the *LEfSe* analyses, we performed higher resolution analyses on the ASV-level. In particular we determined the number, identity and relative abundance of those ASVs which were unique to each sponge microbial cluster.

3. Results

3.1. Phylogenetic and morphological analyses of Phakellia spp.

Our 62 newly sequenced samples formed five well-defined clades corresponding to *Axinella infundibuliformis* and four species of the genus *Phakellia*: *P. rugosa*, *P. ventilabrum*, *P. hirondellei* and *P. robusta* (Fig. 2). *Axinella infundibuliformis* specimens sequenced here were 100% identical and appeared in a moderately supported clade with another *A. infundibuliformis* specimen from Scotland (Morrow et al., 2012) and grouped with other Axinellidea species. The genus *Phakellia* appeared here as polyphyletic. All *P. rugosa* were 100% identical and recovered in a clade with the highest support, together with a *P. rugosa* previously sequenced from Norway (Morrow et al., 2013). *Phakellia ventilabrum* samples formed a monophyletic clade recovered with high support, clustering together with other *P. ventilabrum* specimens as well as with *Axinella cannabina*. The *P. ventilabrum/A. cannabina* clade was sister to a clade comprised of *Axinella*, *Acanthella*, and *Phakellia* representatives (Fig. 2). As for *P. robusta* and *P. hirondellei*, they formed two sister monophyletic clades, with the only *P. hirondellei* clade highly supported (Fig. 2). Interestingly, the *P. robusta* clade was formed by three

monophyletic clades: 1) comprised of individuals from Norway, Kerry Head Reefs, and NW of Orkney with 100% identical sequences, 2) comprised by the Hatton-Rockall Basin closely related with the previous one, and finally 3) an external clade to those that contained specimens from the Cantabrian Sea (Fig. 2). Importantly, all individuals in the first clade of *P. robusta* samples had an intronic region (Cranston et al., 2021).

Specimens of *P. robusta*, *P. hirondellei* and *P. ventilabrum* had combinations of two or three megasclere types: oxeas, strongyles, and styles (Figs. 2 and 3). *Phakellia robusta* (Fig. 3A) had five categories of spicules (Figs. 2, 3B–F): (1) Oxeas I, large, irregularly curved or flexuous sometimes with asymmetrical tips, acerate or mucronate; only one size category with dimensions: 675–(929)–1297 × 28 μm; (2) Oxeas II, short, slightly curved or with a marked angle, points acerate or mucronate; dimensions: 234–(406)–539 x 23–25 μm; (3) Strongyles, large (same size category as oxeas I), flexuous, isodiametric with rounded or sharp ends sometimes different; dimensions: 771–(978)–1286 × 25 μm; (4) Styles I, large, straight or slightly curved and slender; dimensions: 905–(1027)–1320 × 17 μm (this category was more infrequent and was not seen in all specimens); and (5) Styles II, small, slightly curved and fusiform; base hemispherical or rounded and the other tip acerate; dimensions: 337–(551)–790 x 23 μm.

Specimens of *P. hirondellei* from the Cantabrian Sea (Fig. 3G) showed four morphologies of megascleres (Figs. 2, 3H–L): (1) Oxeas I, large, with different degrees of curvature from slightly curved, with a single or double bend to flexuous; tips from slightly blunt to acerate; dimensions: 336–(697)–1551 x 6.2–(13.0)–22.5 μm; (2) Oxeas II, small, slightly curved with tips from acerate to blunt; dimensions: 144–(240)–472 x 3.7–(8.0)–12.5 μm; (3) Styles, slightly curved with acerate ends; dimensions: 191–(482)–1104 x 5.6–(12.0)–17.9 μm; and (4) Strongyles from irregularly curved to flexuous, isodiametric, with rounded ends; dimensions: 1175–(1342)–1543 x 12.1–(12.0)–14.2 μm.

Oxeas I and II were larger in *P. robusta*, being almost twice the size of those in *P. hirondellei*. Strongyles and styles were also longer in *P. robusta*. It is noteworthy that these three spicule types were similar in size in *P. robusta*, while in *P. hirondellei* the strongyles were remarkably larger. Regarding styles, those of *P. robusta* were thinner, longer and could be divided in two categories (large and small), while in *P. hirondellei* only the small size was present and very often they had a clear curvature in the proximal quarter (Figs. 2, 3B–F, H-L).

We also studied the spicules of *Phakellia ventilabrum* (Fig. 3R): they

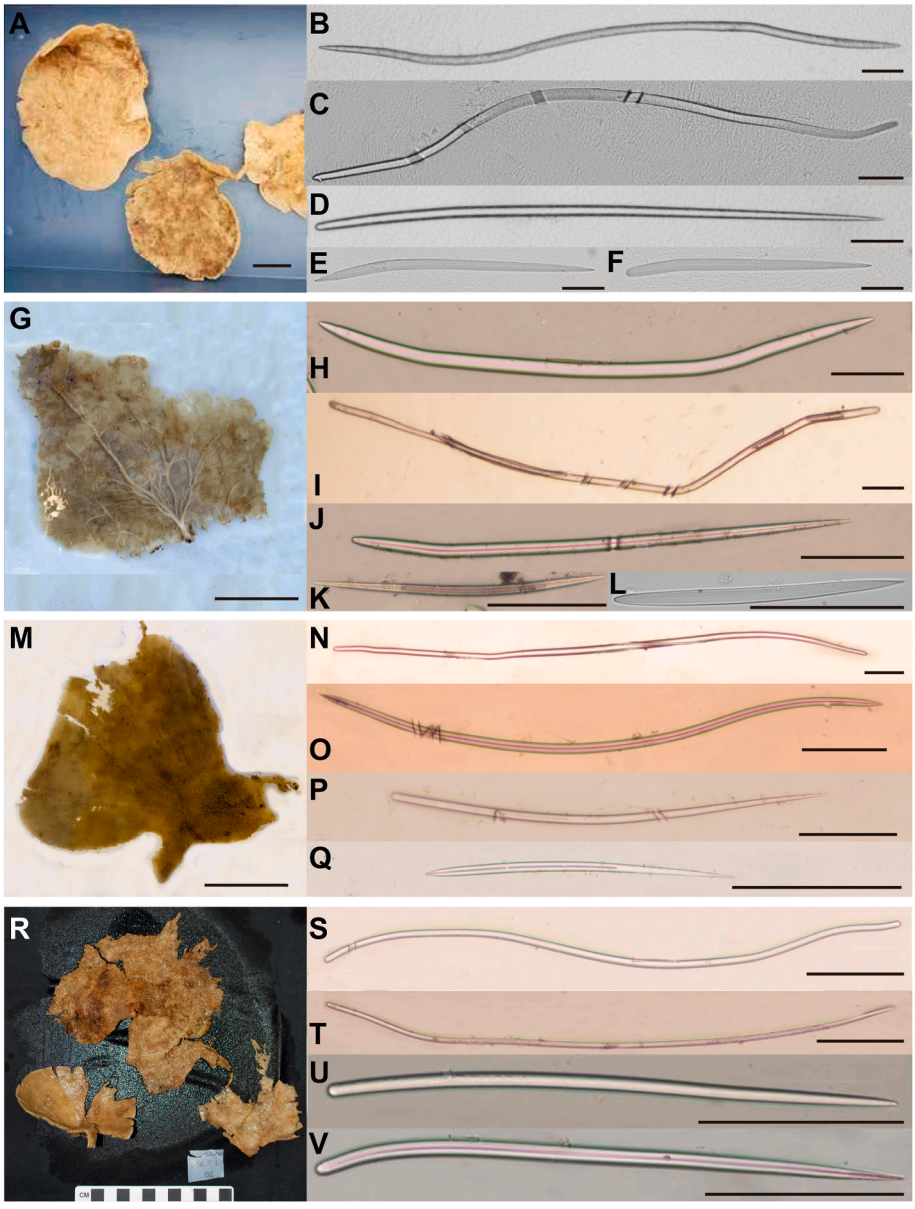

Fig. 3. External appearance and types of megasclere spicules found in *Phakellia* spp. in this study. Scale bars for all spicules 100 μm. **A–F.** *Phakellia robusta*: **A.** Habitus (Prob-Nw-ST6-66), scale bar 2 cm. **B.** Oxea I. **C.** Strongyle. **D.** Style. **E.** Oxea II. **F.** Style II. **G–L.** *Phakellia hirondellei*: **G.** Habitus (Phiron-CS-DR10-458), scale bar 5 cm. **H.** Oxea I. **I.** Strongyle. **J.** Style. **K.** Oxea II. **L.** Style. **M–Q.** *Phakellia* hybrid: **M.** Habitus (Prob-CS-DR14-653), scale bar 2 cm. **N.** Strongyle. **O.** Oxea I. **P.** Style. **Q.** Oxea II. **R–V.** *Phakellia ventilabrum*: **R.** Habitus (Pven-CS-DR2.2), scale bar 12 cm. **S–T.** Strongyles. **U–V** Styles.

showed only two megascleres very different in shape and size (Figs. 2, 3S–V): (1) Strongyles, sinuous to wavy with one, two, three or four inflection points, vermicular appearance, isodiametric with hemispherical endings and sometimes with unequal ends; dimensions: 457–(721)–848 x 5.9–(6.8)–8.3 μm; and (2) Styles, straight, slightly curved or with a basal bend in the proximal third or fourth; base rounded, hemispherical and the other end pointed to acerate; dimensions: 227–(272)–345 x 6.5–(7.4)–8.5 μm.

3.2. Population structure and connectivity using COI

The haplotype network for *P. hirondellei* and *P. robusta* (Fig. 4) was done with 148 homologous sites, resulting in the two species being clearly separated by three mutational steps (K2P and *p*-distance of 2.7±1.2 and 2.6±1.2%, respectively). Interestingly, we observed genetic structure in *P. robusta*, with samples from deeper locations (Prob-HRB-S15, Prob-CS-DR7, and Prob-CS-DR14) being clearly separated from the rest of shallow-water samples (locations Prob-Nw, Prob-KHR, Prob-Ork-H045) (Fig. 4). While only one haplotype was found in the shallow-water *P. robusta*, three haplotypes were identified from the deep-sea samples of *P. robusta* (Fig. 4), two in Hatton-Rockall Basin (Prob-NRB-S15) and one in the Cantabrian Sea (Avilés Canyon System –Prob-CS-DR14– and *El Cachucho* MPA –Prob-CS-DR7–). Contrastingly, *P. hirondellei* did not show any genetic structure (Fig. 4), although in this case samples were collected from a quite limited geographic area spanning less than 100 km (Fig. 1; Table 1).

3.3. Population structure and connectivity using neutral SNPs

Population genetics statistics for *P. robusta* is indicated in Table 2. Overall expected heterozygosity (H_e), generally considered as a measure of genetic diversity, was relatively low for *P. robusta* (0.177), with values by region ranging from 0.143 (Kerry Head Reefs) to 0.194 (Hatton-Rockall Basin). Overall observed heterozygosity (H_O) was again relatively low for *P. robusta* (0.159), with values by region ranging between 0.118 (Kerry Head Reefs) and 0.179 (Cantabrian Sea). All values for the inbreeding coefficient (F_{IS}) were positive but close to zero, indicating a slight excess of observed homozygotes; an exception was the F_{IS} for the Cantabrian Sea that was −0.029.

A strong genetic structure was detected for *P. robusta* (Fig. 5; Suppl. Mat.1 A–D). The optimal number of clusters detected by *STRUCTURE* was two (k =2) followed by three (k = 3) (Fig. 5, Suppl. Mat.1 A). Results for k = 2 in *P. robusta* revealed two major clusters grouping samples per bathymetric range (Fig. 5A): the Red Cluster, comprised by samples collected from the Cantabrian Sea (Prob-CS-DR7 and Prob-CS-DR14) and the Hatton-Rockall Basin (Prob-HRB-S15); and the Blue Cluster, including samples from Norway (Prob-Nw), NW of Orkney (Prob-Ork) and Kerry Head Reefs (Prob-KHR). This differentiation of samples in two clusters matched with a bathymetric segregation of samples, with samples from the Red Cluster found at depths of 340–1,150 m, while samples from the Blue Cluster occurring between 29 and 332 m (Fig. 5B; Table 1). When plotting the *STRUCTURE* analysis for k=3, the second most likely number of clusters for the dataset (Suppl. Mat.1 A), the Cantabrian Sea samples were identified as a different cluster (Orange Cluster), and some introgression of this cluster was identified in the individuals Prob-HRB-S15-13-1-2, Prob-Nw-ST5-48, and Prob-Nw-ST6-63 (Fig. 5B).

Similarly as for the *STRUCTURE* analysis, our results for *snapclust* and *DAPC* for the *P. robusta* dataset also detected two (k = 2) and three (k = 3) as the most likely number of clusters (Suppl. Mat.1 A–B). The *DAPC* analysis for k =2 identified the same two major clusters identified in the *STRUCTURE* analysis grouping samples per bathymetric range (Suppl. Mat.1 C–D), while the *DAPC* for k = 3 also grouped apart samples from the Cantabrian Sea, the Hatton-Rockall Basin and the shallow-water *P. robusta* including those from Kerry Head Reefs, NW of Orkney, and Norway (Fig. 5C).

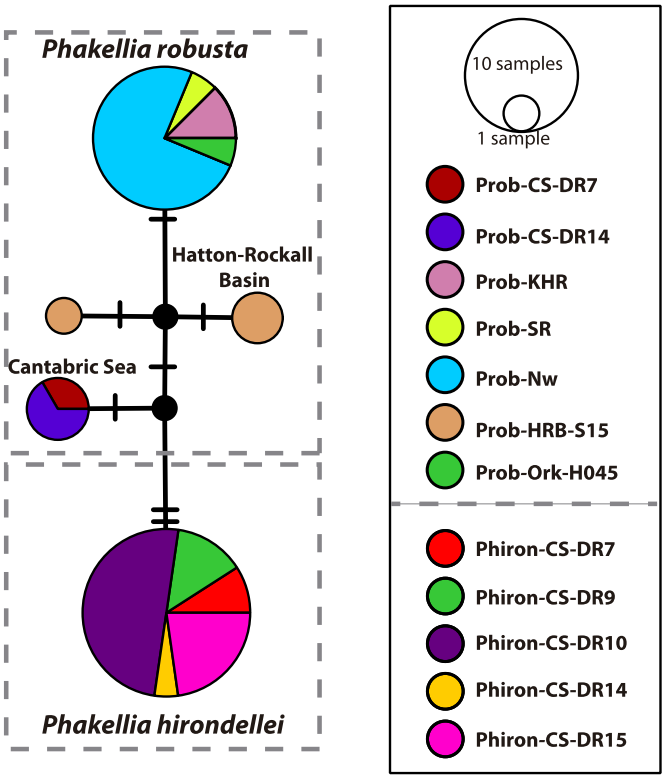

Fig. 4. *COI* haplotype networks for *Phakellia robusta* and *P. hirondellei* (colour coding by sampling station). Circles are proportional to the number of individuals for each haplotype. Number of mutations between haplotypes is indicated with crossed lines and missing inferred haplotypes are in black. (For interpretation of the references to colour in this figure legend, the reader is referred to the Web version of this article.)

Pairwise F_{ST} comparisons for *P. robusta* grouping the samples per region found moderate (0.179–0.310) to high (0.515–0.540) values (Table 3). These F_{ST} values were the highest when comparing deep-water regions (Cantabrian Sea and Hatton-Rockall Basin) to shallow-water ones (Kerry Head Reefs and Orkney-Norway) and the lowest when comparing stations within deep- and shallow-water regions. Significant pairwise F_{ST} values were only found between Orkney-Norway and the rest of regions (Table 3).

AMOVA results grouping samples per region and bathymetric range (deep *vs* shallow-water) found significant differences in the genetic structure between the different regions and bathymetric ranges, explaining ca. 50% of the total variance (p-value < 0.01) in both cases (Table 4).

The results of the *Barrier* analysis for *P. robusta* supported the genetic structure observed in our *STRUCTURE* analysis, identifying three relevant genetic barriers separating the four regions mentioned above (Suppl. Mat. Fig. 2A). The three genetic breaks were: (1) between Cantabrian Sea and the rest of regions; (2) between Hatton-Rockall Basin and the rest of regions; and (3) between Orkney-Norway and the rest of regions (Suppl. Mat. Fig. 2A). Finally, the only significant asymmetric

Table 2
Population genetics statistics for *P. robusta*. Samples grouped by region. H_o observed heterozygosity, H_e expected heterozygosity, F_{IS} inbreeding coefficient.

Region	H_O	H_e	F_{IS}
Cantabrian Sea	0.179	0.174	−0.029
Kerry Head Reefs	0.118	0.143	0.174
Hatton-Rockall Basin	0.149	0.194	0.230
Orkney-Norway	0.153	0.171	0.106
Total *P. robusta*	0.159	0.177	0.102

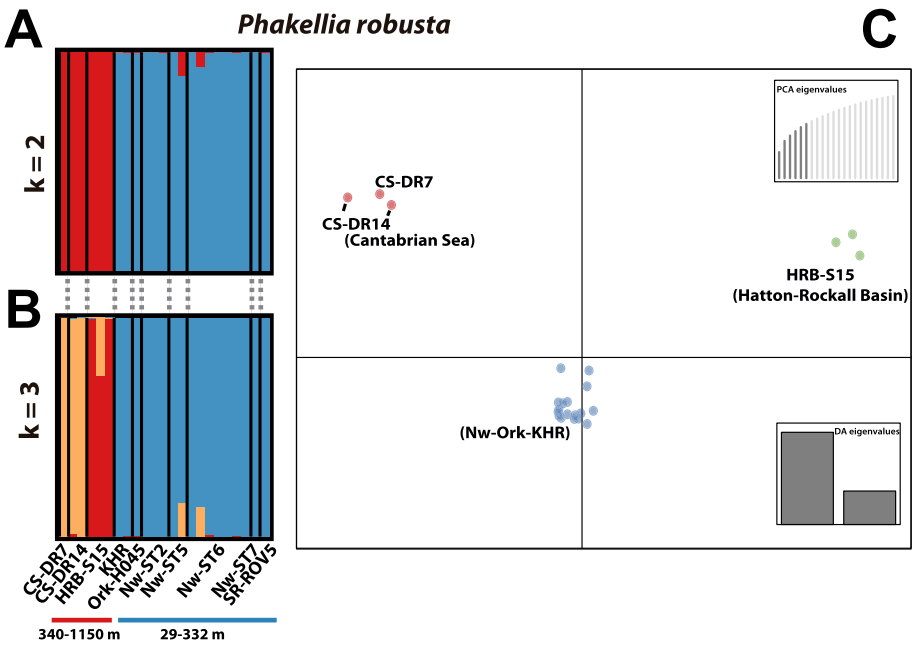

Fig. 5. A. Individual genotype assignment of *P. robusta* to clusters (K) as inferred by *STRUCTURE* for all studied sites with k=2. **B.** Individual genotype assignment of *P. robusta* to clusters (K) as inferred by *STRUCTURE* for all studied sites with k=3. Depth range for sampling sites is indicated at the bottom figure. C. *DAPC* analysis of *P. robusta* assigning samples to k=3 as inferred by the function *snapclust*.

migration detected for *P. robusta* was observed from the Kerry Head Reefs to Orkney-Norway (Suppl. Mat. Fig. 2B).

3.4. Hybridization between P. robusta and P. hirondellei: signals from the genome, the phenotype, and the microbial community composition

When we analysed the SNP dataset of *P. robusta–P. hirondellei* together, striking results appeared in the population assignment plots of *STRUCTURE* (Fig. 6A). The optimal number of clusters detected was two (k =2) followed by three (k = 3) (Suppl. Mat. Fig. 3A). Results for k = 2 in the combined dataset identified two major genotypic clusters grouping samples that were not entirely coincident with the two species detected in the phylogenetic tree or using morphological analyses of spicules (Figs. 2–3, 6A): (a) Blue Cluster, with samples of *P. robusta* from NW of Orkney and Norway; and (b) Purple Cluster, with most of the individuals from *P. hirondellei* plus samples of *P. robusta* from deep-water stations (Prob-CS-DR7, Prob-CS-DR14), all with approx. 100% of population assignment. In some individuals of both species we detected some degree of introgression between the two clusters (Fig. 6A): samples from the deep-sea population of Hatton-Rockall Basin with *P. robusta COI*, showed about 80% assignment to the Purple Cluster (Fig. 6A), while some samples of *P. hirondellei* showed approximately 40–60% assignment to the two clusters (Fig. 6A). Very minor introgression was also detected in some *P. robusta* samples from the Cantabrian deep-sea (Fig. 6A).

Our results for *snapclust* for the combined dataset detected three different clusters (k = 3), again not entirely coincident with the morphological and phylogenetic results for the two species (Figs. 2 and 6B, Suppl. Mat. Fig. 3B–D): one cluster was composed by *P. hirondellei* specimens; another cluster was composed by samples of *P. robusta* from shallow-waters (Kerry Head Reefs, NW of Orkney, and Norway); and another cluster was composed of *P. robusta* from deep waters (Cantabrian Sea and Hatton-Rockall Basin). Interestingly, the hierarchical Ward clustering on the allele data using the combined dataset showed *P. robusta* from the deep-water stations as sister to *P. hirondellei* samples (Suppl. Mat. Fig. 3D).

To further investigate the potential occurrence of hybridization (or

Table 3
Pairwise F_{ST} values for samples of *P. robusta* grouped by region. Significant values in bold. Regions included in the analyses are Cantabrian Sea, Kerry Head Reefs (SW Ireland), Rockall Plateau (Hatton-Rockall Basin), and Orkney-Norway, the latter considering samples collected from Korsfjorden, Sula Reef, and NW of Orkney in the same group.

	Cantabrian Sea	Kerry Head Reefs	Hatton-Rockall Basin	Orkney-Norway
Cantabrian Sea	–			
Kerry Head Reefs	0.540	–		
Hatton-Rockall Basin	0.310	0.539	–	
Orkney-Norway	**0.515**	**0.179**	**0.530**	–

Table 4
Results of the *AMOVA* analysis for *P. robusta* grouping sample per region and by depth ranges. *d.f.* degrees of freedom. Significant *p*-values in bold. See Table 1 for sample assignation to the different regions ('Region' column) and depths (Shallow: including Kerry Head Reefs, Korsfjorden, Sula Reef, and NW of Orkney; Deep: including Cantabrian Sea and Hatton-Rockall Basin). Regions included in the analyses are: Cantabrian Sea, Kerry Head Reefs (SW Ireland), Rockall Plateau (Hatton-Rockall Basin), and Orkney-Norway, the latter considering samples collected from Korsfjorden, Sula Reef, and NW of Orkney in the same group.

Source of variation	d. f.	Sum of squares	Fixation Index	% variation	*p*-value
Among Regions	3	65.254	FCT: 0.4901	49.02	**0.0008**
Among Locations within Regions	6	10.99	FSC: 0.09514	−4.85	0.9098
Within Locations	36	101.06	FST: 0.44168	55.83	**0.0003**
Among Depths	1	51.53	FCT: 0.48662	48.66	**0.0089**
Among Locations within Depths	8	24.715	FSC: 0.02364	1.21	0.4561
Within Locations	36	101.06	FST: 0.49875	50.12	**0.0003**

introgression), we simulated hybrids using *hybridize*, and then analysed them together with the SNP dataset from *P. robusta* and *P. hirondellei* using a *DAPC* analysis (Fig. 7A). Three clusters were identified: one containing all shallow-water *P. robusta* individuals, another with most of *P. hirondellei* individuals, and then an intermediate cluster with the simulated hybrids, the six deep-water *P. robusta* individuals (Prob-CS-DR14-651, Prob-CS-DR14-653, Prob-CS-DR7-244, Prob-HRB-S15-13, Prob-HRB-S15-13-1-2, and Prob-HRB-S15-13-2-2), and five individuals of *P. hirondellei* (Phiron-CS-DR7-251, Phiron-CS-DR9-383, Phiron-CS-DR10-470, Phiron-CS-DR15-856, and Phiron-CS-DR15-857e: the same individuals with a significant amount of introgression identified in the *STRUCTURE* analysis in Fig. 6A, except for sample Phiron-CS-DR9-383, identified in the Blue Cluster in the *STRUCTURE* analysis). Our results using *fineRADstructure* strongly supported those of *adegenet hybridize*, identifying the same potential hybrids mentioned above in the *hybridize* analysis (Fig. 7B).

Morphologically, we detected mixed features in only the deep-sea individuals of *P. robusta* (identified as such using *COI*), from the Cantabrian Sea and Hatton-Rockall Basin (Figs. 2 and 3). However, those individuals of *P. hirondellei* with signs of introgression did not apparently show mixed spicules. The spicules of these hybrid individuals from Hatton-Rockall Basin and the Cantabrian Sea (Fig. 3M) showed intermediate characters between *P. robusta* and *P. hirondellei* (Figs. 2 and 3) in the four morphologies of megascleres observed (Fig. 3N–Q): (1) Oxeas I, large, curved, sinuous and thick; dimensions: 427–(703)–1185 x 5.2–(11.0)–19.1 μm; (2) Oxeas II, short, thick, straight but slightly curved; dimensions: 149–(195)–285 x 5.0–(6.3)–8.6 μm; (3) Strongyles, long and sinuous; dimensions: 1175–(1342)–1542 x 12.1–(12.8)–14.2 μm; and (4) Styles, straight or slightly curved; dimensions: 333–(516)–1428 x 6.5–(9.2)–13.4 μm. These individuals of *Phakellia* (hybrids) had styles I and II similar in shape and size to the ones in *P. hirondellei* and with clear differences with those in *P. robusta*, which have syles I straight and longer (double the length in *P. robusta*). However, strongyles in *Phakellia* hybrids were similar in size to the ones in *P. robusta*, and differed from the smaller and more sinuous strongyles in *P. hirondellei*. As for Oxeas I, they were larger in *P. robusta* (almost double the size of those in *P. hirondellei* and the hybrids), and more robust in *P. hirondellei* than those in the hybrids.

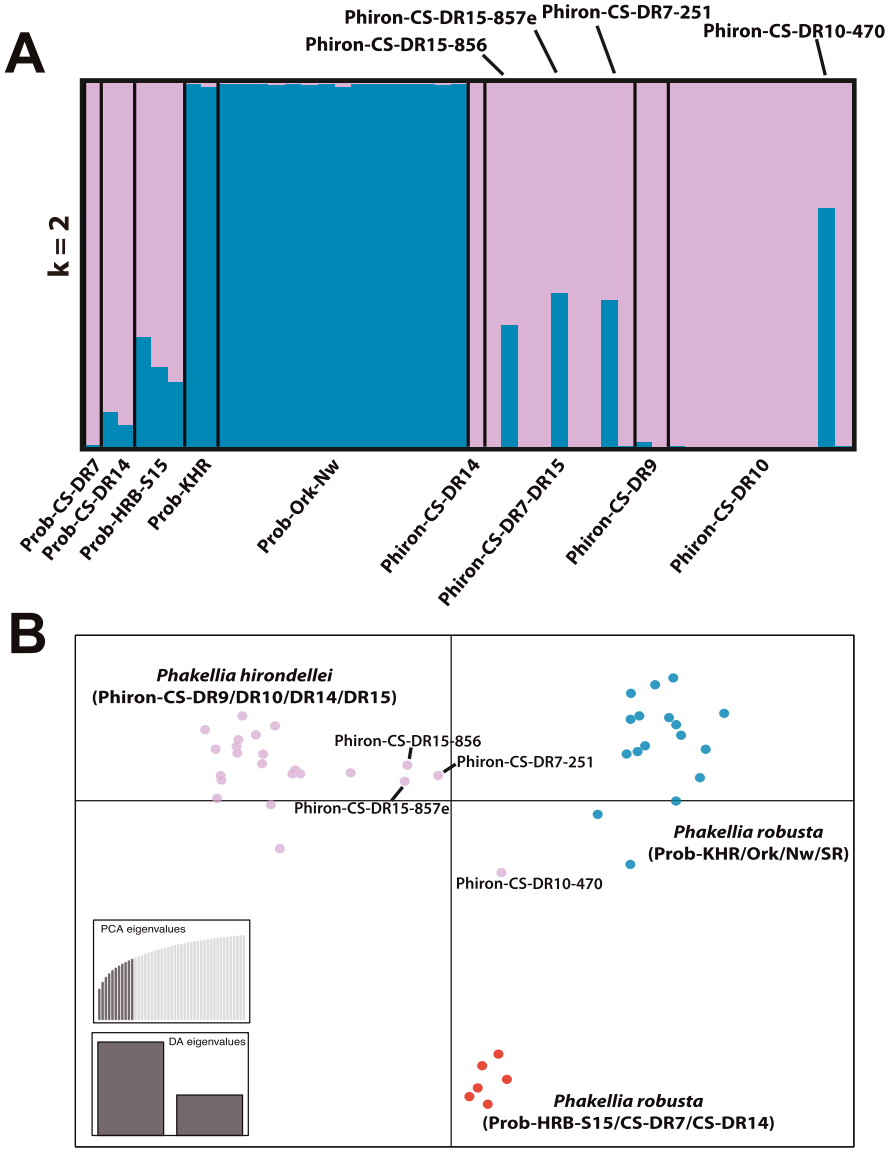

Fig. 6. Combined analysis of *P. hirondellei* and *P. robusta* **A.** Individual genotype assignment of individuals to clusters (K) as inferred by *STRUCTURE* for all studied sites with k=2. **B.** *DAPC* assigning samples to k=3 as inferred by the function *snapclust*.

Finally, the evidence from the distance (*UniFrac*) analysis of the microbial community composition of *P. robusta* and *P. hirondellei* was also not coincident with our results from the phylogenetic analyses since we recovered four different clusters (Fig. 8): Cluster A, composed of a mixture of *P. robusta* samples from the shallow waters of Kerry Head Reefs, NW of Orkney, and Norway; Cluster B, comprising all the samples of *P. robusta* from Norway (except for Prob-SR-ROV5-13 and Prob-Nw-ST-6A, present in Cluster A) and one of the samples from Kerry Head Reefs (Prob-KHR-21); Cluster C, composed by the three *P. robusta* samples from Hatton-Rockall Basin; and Cluster D (sister to Cluster C), comprising all the samples from *P. hirondellei* and the three specimens of *P. robusta* from the Cantabrian Sea (Prob-CS-DR7-244, Prob-CS-DR14-651, and Prob-CS-DR14-653). In general, grouping by sampling station was not detected except for the cases of members of Cluster C (all of them belonging to the same deep-water station) and the three specimens from station DR14 in the Cantabrian Sea (one *P. hirondellei* specimen, and two *P. robusta* specimens). Importantly, the sample of *P. ventilabrum* from station DR14 (Pventi-Cs-DR14-650) displayed a distinct microbial community when compared to the two specimens of *P. robusta* also collected from the same station (Prob-Cs-DR14-651 and 653). Similarly, the samples of *Axinella infundibuliformis* (Ainf-Nw-ST5-45) and *Phakellia rugosa* (Prug-Nw-ST5-41) included also in our microbial analysis, also displayed a different microbial community composition when compared to *P. robusta* specimens collected from the same location (Prob-ST5). Despite distinct signatures at the ASV-level, the microbial community composition of all analysed sponge species showed a prevalence of mainly the same microbial phyla with a dominance of Proteobacteria, Nitrospirae, and Actinobacteria (Fig. 8). Major differences between the community compositions of samples were attributed to the relative abundances of the different phyla (Suppl. Mat. Fig. 4A): in Cluster A Bacteroidetes were the most enriched, in Cluster B Proteobacteria, in Cluster C Actinobacteria, and in Cluster D Gemmatimonadetes. On a higher resolution, we detected 25 ASVs (belonging to the significantly enriched phyla shown in Suppl. Mat. Fig. 4A) which were unique to the different sponge microbial clusters (Suppl. Mat. Fig. 4B).

4. Discussion

4.1. Systematics of Phakellia spp.

The genera *Phakellia*, *Acanthella*, and *Axinella* are particularly problematic from a taxonomic point of view (Álvarez and Hooper, 2002), given their extremely reduced spicule complement and the convergent shape habitus. The genus *Phakellia* currently comprises 34 accepted species (Van Soest et al., 2020), although several species present serious morphological divergences that challenge their taxonomic affiliation (Carvalho et al., 2007). We focused here entirely in the relationships between *Phakellia robusta* and *Phakellia hirondellei*. Interestingly, *P. hirondellei* was presented in a preliminary note (Topsent, 1890) with this name but later described within the genus *Tragosia* (Topsent, 1892). Much later, Topsent described it merely as a variety of *Phakellia robusta* var. *hirondellei* (Topsent, 1928), highlighting that *P. robusta* and *P. hirondellei* are in fact morphologically very similar and therefore difficult to distinguish. Indeed, both species have oxeas, strongyles and styles as structural elements of their skeleton, although some basic differences were presented here regarding the size and morphology of these spicules (see Figs. 2 and 3). Our phylogenetic analyses corroborated these morphological similarities (Figs. 2 and 3), by placing them as sister groups, although with only moderate support (Fig. 2). Indeed, *COI* genetic distances reported here between *P. robusta* and *P. hirondellei* were relatively low (K2P and *p*-distance of 1.9±0.7%), especially when compared to the variability found between these two species and *P. ventilabrum* (K2P and *p*-distance values > 13%). The genetic distances reported between *P. robusta* and *P. hirondellei*, though, are comparable to what has been reported for other studies comparing closely related congeneric species (Huang et al., 2008; Pöppe et al., 2010). But the most interesting results we obtained are the past events of hybridization we detected between these two clades, which is discussed below.

4.2. Genetic diversity and molecular connectivity in Phakellia spp.

Mitochondrial markers (e.g. *COI*) usually provide very little resolution for population genetics studies of sponges (see Pérez-Portela and Riesgo 2018). Even when studying samples collected from locations separated by hundreds of km, *COI* has been shown to have no variation for both shallow and deep-water sponge species (Leiva et al., 2019; Pérez-Portela and Riesgo, 2018; Taboada et al., 2018). In turn, other markers such as SNPs (e.g. Brown et al., 2017; Leiva et al., 2019) or microsatellites (e.g. Dailianis et al., 2011; Pérez-Portela et al., 2015; Chaves-Fonnegra et al., 2015; Riesgo et al., 2016, 2019; Taboada et al., 2018) have the power to detect genetic structure in sponges. Following the general pattern for sponges, the *COI* from *P. hirondellei* displayed no variability for the samples studied (Fig. 4). Contrastingly, the *COI* from *P. robusta* showed variability when comparing samples collected at the deep-water locations (Prob-HRB-S15, Prob-CS-DR7, and Prob-CS-DR14) with those from shallow waters (Fig. 4). However, it is important to note that the sampling breadth for *P. robusta* was higher than for *P. hirondellei*, with samples of *P. hirondellei* spanning less than 100 km while samples of *P. robusta* were more than 3,000 km apart (Fig. 1).

As already anticipated, ddRADseq-derived SNPs generated for *P. robusta* provided a finer-scale resolution on the molecular connectivity across the study area. In *P. robusta*, and similar to our results from the *COI* analysis, a clear genetic segregation was observed between samples from deeper stations (Prob-HRB-S15, Prob-CS-DR7, and Prob-CS-DR14) and those from shallower stations, despite the latter grouping samples more than 2,000 km apart (Prob-KHR respect to Prob-SR-ROV5) (Figs. 1A, 5A–C). Interestingly, asymmetric contemporaneous migration was detected from Kerry Head Reefs to NW of Orkney/Norway. This pattern might be explained by prevalent oceanographic currents running from the area of the British Isles to the North Sea, where the Eastern North Atlantic Central Water runs northwards to meet the Norwegian Coastal Current (Castrillejo et al., 2018; Hansen and Østerhus, 2000; Storesund et al., 2017).

Our results for *P. robusta* echo those seen in other deep-sea marine invertebrates –including both mobile and sessile fauna– that gene flow in deep-sea organisms is driven predominantly by bathymetry (vertical) rather than geographical (horizontal) distances (e.g. France and Kocher 1996; Quattro et al., 2001; Zardus et al., 2006; Clague et al., 2012; O'Hara et al., 2014), including another deep-sea demosponge (Taboada et al., 2018). In some cases, genetic differences observed among depth regimes were suggested to be due to the presence of cryptic lineages (e.g. France and Kocher 1996; Quattro et al., 2001; Zardus et al., 2006; Schüller 2011), something that should be ruled out for the case of *P. robusta*. Alternatively, processes of introgression derived from hybridization between the two species (see below) might be present, a phenomenon that has already been suggested as a potential factor contributing to the genetic structure between sponge populations (Pérez-Portela and Riesgo, 2018).

4.3. Hybridization in Phakellia species

One of the most remarkable results of our study is the presence of hybrid individuals, which were assigned to either *P. robusta* or *P. hirondellei* based on the different features and markers used (Figs. 2, 6A and 7).

The signals of hybridization were not only restricted to the genomes

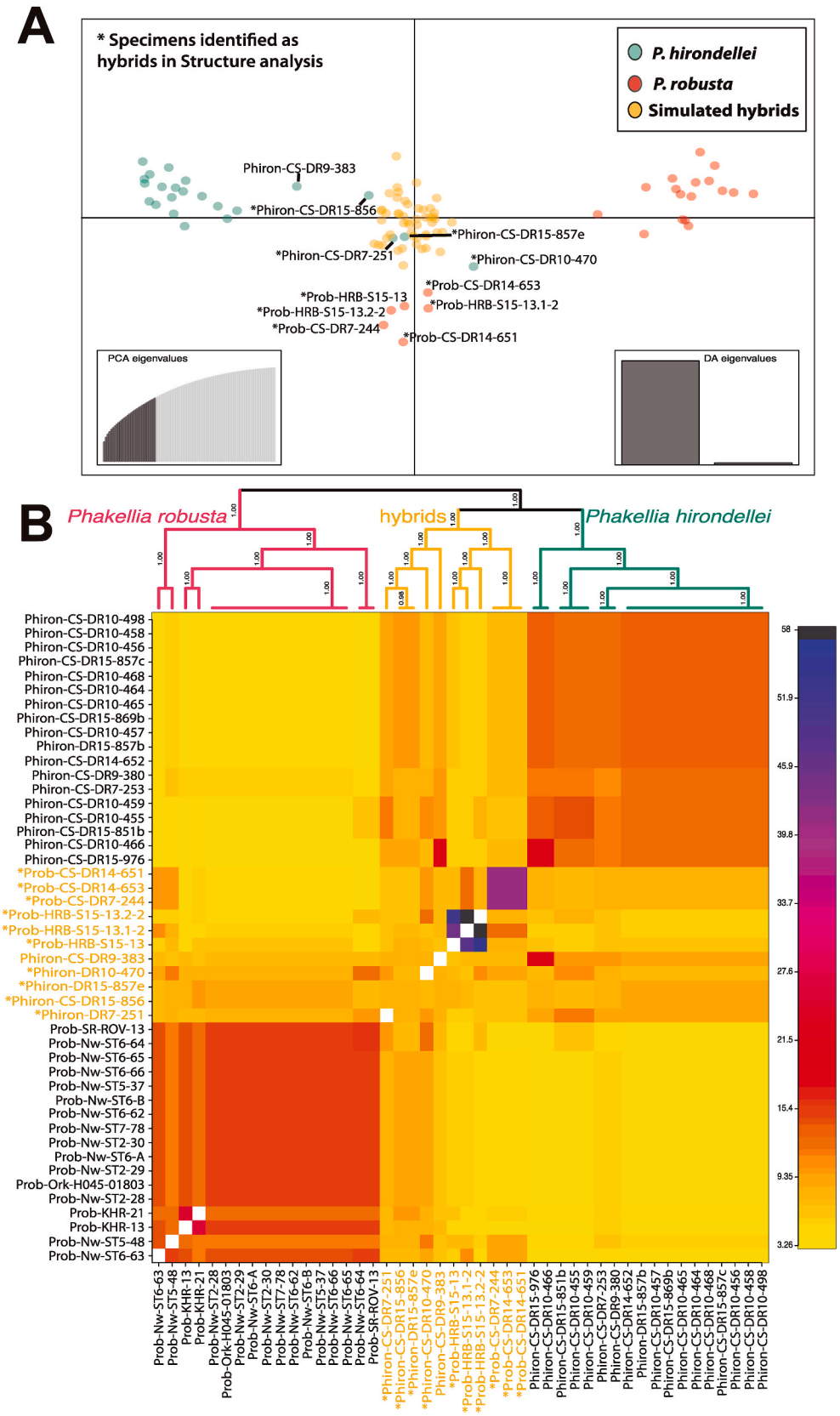

Fig. 7. A. *DAPC* analysis showing *P. hirondellei* specimens (green), *P. robusta* specimens (red), and simulated hybrids (yellow) between the two species. **B.** Simple co-ancestry matrix obtained from the *fineRADstructure* analysis. Asterisks indicate specimens identified as potential hybrids in Fig. 6A. (For interpretation of the references to colour in this figure legend, the reader is referred to the Web version of this article.)

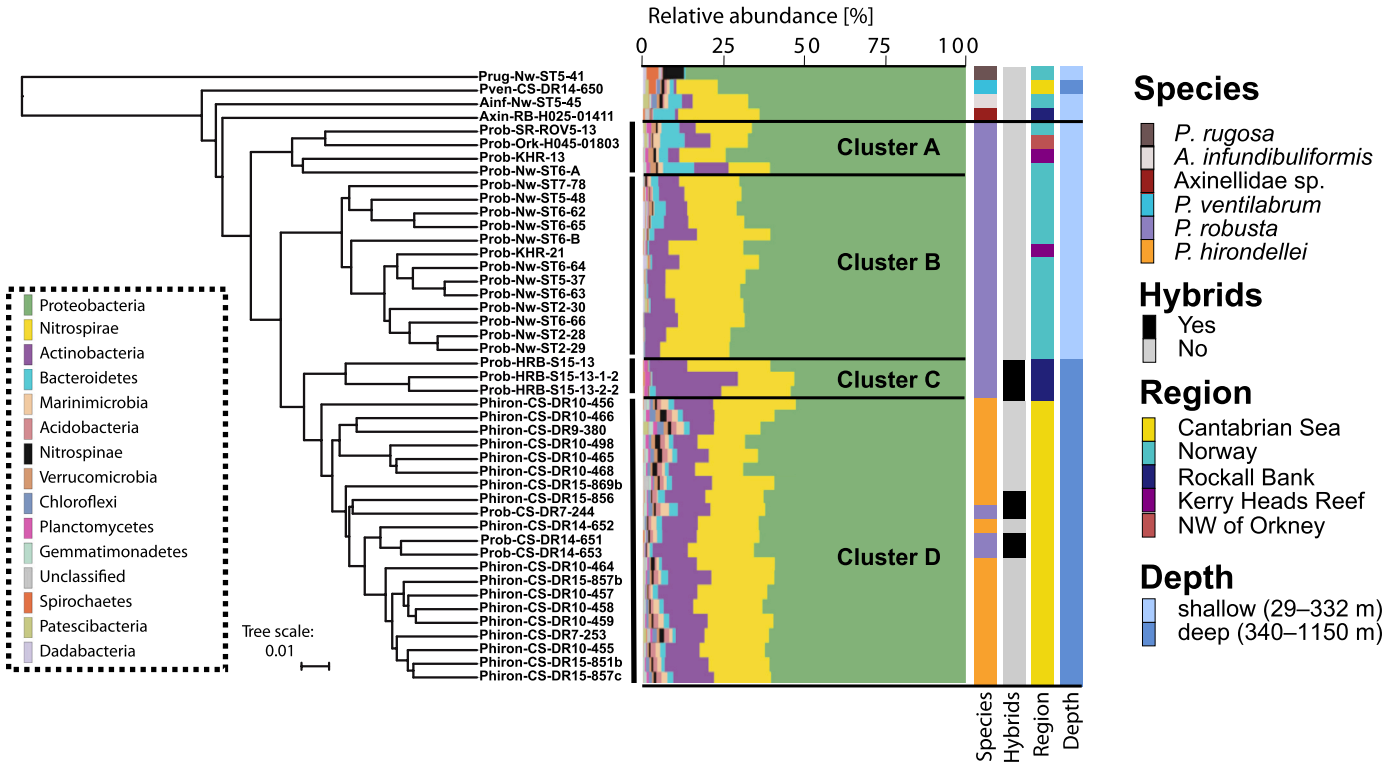

Fig. 8. Clustering dendrogram in combination with a barchart, showing similarities of microbial communities between sponge individuals and relative abundances of the 15 most abundant microbial phyla across the different sponge samples. The clustering dendrogram is based on weighted *UniFrac* distances (ASV-level). Clusters (A, B, C, D) were determined by visual inspection of the dendrogram. Microbial phyla are sorted in the legend (bottom left) in decreasing order after their mean relative abundance. Four colour codes are added at the most right side for all sponge samples, indicating species affiliation, hybrid status, sampling region, and depth range. (For interpretation of the references to colour in this figure legend, the reader is referred to the Web version of this article.)

(nuclear or mitochondrial) of the sponges, but they expanded to their microbial community compositions. Sponges are generally considered as holobiont organisms, and they display rather complex symbiotic relationships with bacteria (Pita et al., 2018). Sponge species are broadly categorized as either Low or High Microbial Abundance (LMA or HMA) depending on the abundance of the extracellular bacteria they harbour within their tissues (Gloeckner et al., 2014; Hentschel et al., 2006). The sponge microbial community is considered to be host species-specific, even though communities are exceedingly complex with a mix of generalist bacteria (detected in other sponge species from other geographic areas) and specialist bacteria (more prevalent in some species and rare or absent in others) (Erwin et al., 2012; Thomas et al., 2016). *Phakellia* species are LMA sponges without known vertical transmission of bacteria (Koutsouveli et al. in preparation), which suggests that the specific symbiotic community is not inherited through the reproductive stages (Hentschel et al., 2012; Webster et al., 2010). As expected, the *UniFrac* distance analysis of the microbial communities of *P. robusta* and *P. hirondellei* separated samples from the two species in four groups that did not entirely correspond to the phylogenetic assignment (Fig. 8). Interestingly, the deep-water specimens of *P. robusta* from Hatton-Rockall Basin and those from the Avilés Canyon System and *El Cachucho* MPA were identified phylogenetically as *P. robusta* (Fig. 2), but their microbial community composition was more similar to that in *P. hirondellei* (Fig. 8). The results for the microbial composition are therefore similar to those from the *STRUCTURE* analysis of the host, with samples of *P. robusta* from these deep-water areas showing more affinities to *P. hirondellei* (Fig. 6A). These mixed signals are in agreement with our identification of these deep-water *P. robusta* specimens as potential hybrids between *P. robusta* and *P. hirondellei* (Fig. 7A–B).

Here, we suggest that a past introgression event occurred between *P. robusta* and *P. hirondellei*, resulting in the lateral exchange of microbial communities, which could explain the presence of hybrids detected in our study. Although interspecific symbiont exchange is completely unknown for sponges, it has recently been reported in two sympatric deep-sea vesicomyid clams. In their study, Breusing et al. (2019) inferred that *Archivesica gigas* (Dall, 1896) and *Phreagena soyoae* (Okutani, 1957), which are known to transmit their symbionts vertically, hybridized in the past probably after an event of lateral transmission between the species. Our results suggest a similar albeit more complex scenario for *P. robusta* and *P. hirondellei*, because in our case there is no vertical transmission of symbionts. The microbial community of the hybrids originally identified phylogenetically as *P. robusta* was more similar to *P. hirondellei*, which largely matches the assignment of individuals using nuclear SNPs (Fig. 6A). We hypothesize that these hybrids are the result of the crossing between a mother *P. robusta* (the reason why the mitochondrial information is coincident with *P. robusta*) and a father *P. hirondellei*. This might be the reason why a *COI* intronic region has only been detected in the shallow-water specimens of *P. robusta* and not in the deep-water *P. robusta* hybrids (Cranston et al., 2021).

This is counter to what we observed in the *P. hirondellei* hybrids, which did not show any difference in the *COI* or the spicule composition and arrangement in respect to the non-hybrid *P. hirondellei* (Figs. 2 and 3). In this case, hybridization might have occurred between a mother

P. hirondellei and a father *P. robusta*. Unfortunately, only one hybrid of *P. hirondellei* (Phiron-CS-DR15-856) was included in the microbial analysis (Fig. 8), preventing us from extracting any further conclusion based on this analysis. In any case, all this indicates that hybridization between *P. robusta* and *P. hirondellei* might have occurred at least two times. Our data are therefore more consistent with horizontally transmitted microbiota in *P. robusta* hybrids that were selected and filtered using the battery of immune genes or alleles more consistent with the nuclear genome of *P. hirondellei*. Host-microbe associations are considered drivers of evolutionary innovation (Margulis and Dorion, 2008; McFall-Ngai et al., 2013) and now are seen as motors of speciation (Brucker and Bordenstein, 2012). In this context, the occurrence of hybrid species with an "exchanged" microbial community could be potentially indicating an undergoing speciation process, given that the host immune system might have changed to adjust to the microbiota.

Hybridization in the seas is not an uncommon phenomenon. The relatively smaller number of examples of introgression in marine organisms as compared to terrestrial organisms is probably more related to the difficulty in collecting/observing marine organisms (Arnold and Fogarty, 2009). Reef corals, though, have a wealth of examples describing introgressive hybridization leading to a combined enrichment of genetic and morphological variation, which has been instrumental, for instance, in the diversification of species of the genus *Acropora* on evolutionary timescales (see Willis et al., 2006). Contrastingly, there is little information about hybridization in sponges, where, to our knowledge, hybridization has only been documented for the shallow-water species *Ircinia fasciculata* and *I. variabilis* (Riesgo et al., 2016). For these closely-related Mediterranean sponges, microsatellites revealed the presence of hybrids in some of the locations studied with a predominant directionality of gene flow observed from one species (*I. variabilis*) to the other (*I. fasciculata*), similar to what we observed between *P. hirondellei* and *P. robusta*. Whether hybridization is a common phenomenon for sponges is still unknown although, given the oviparous nature of many sponges, coupled with the apparent lack of gamete recognition systems in many of them (Maldonado and Riesgo, 2009), we anticipate that it might be quite common. The increasing use of next-generation techniques to study hybridization and speciation processes (Seehausen et al., 2014), successfully applied to other marine invertebrates (Bouchemousse et al., 2016; Breusing et al., 2019; Fraïsse et al., 2016), will most likely help to uncover these processes in sponges too, especially for closely related species, for which it has been predicted that genetic introgression might be more common than expected (Fraïsse et al., 2016).

4.4. Conservation implications

Particularly noteworthy is that the two types of hybrids between *P. robusta* and *P. hirondellei* were detected in *El Cachucho* and the Hatton-Rockall Basin MPAs (Prob-CS-DR7, Prob-CS-DR14, and Prob-HRB-S15). It remains to be further tested, though, in which areas (apart from the ones identified in our study) hybrids are predominately present and if they occur in hybrid zones as it has already been established for other marine species (e.g. Won et al., 2003; Harper and Hart 2007). It also remains to be investigated which potential evolutionary advantages (if any) hybrids may have. At least for *P. robusta* hybrids, the genetic diversity values were slightly higher when compared to *P. robusta* non-hybrids (Table 5), but other advantages such as the acquisition of new traits and/or heterosis (*i.e.* hybrid vigour) may also play a role for the emerging species (Willis et al., 2006). Future analyses including a more balanced sampling effort will allow us to compare the effectiveness of area-based management tools (such as MPAs) or closure areas in protecting the genetic diversity of these and other habitat-forming species. In any case, conservation strategies should not only consider genetic diversity, molecular connectivity patterns and turnover at the population level of key species when planning conservation and management plans (Baco et al., 2016), but should also consider the protection of hybridizing species given the important role they play in generating taxonomic novelty (Ennos et al., 2005).

Table 5
Population genetics statistics for *P. robusta* and *P. hirondellei* distinguishing between hybrids and non-hybrids for both species separately. H_o observed heterozygosity, H_e expected heterozygosity, F_{IS} inbreeding coefficient.

Species/Hybrid	H_O	H_e	F_{IS}
P. robusta-Hybrid			
Prob-Non Hybrid	0.139	0.147	0.055
Prob-Hybrid	0.251	0.211	−0.194
P. hirondellei-Hybrid			
Phiron-Non Hybrid	0.134	0.235	0.428
Phiron-Hybrid	0.125	0.13	0.037

Funding

The work leading to this publication has received funding from the European Union's Horizon 2020 research and innovation programme through the SponGES project (grant agreement no. 679849). This document reflects only the authors' view and the Executive Agency for Small and Medium-sized Enterprises (EASME) is not responsible for any use that may be made of the information it contains. ST received funding from funding from the grant PID2020-117115GA-100 funded by MCIN/AEI/10.13039/50110001103 and also received funding from the Juan de la Cierva-Incorporación program (IJCI-2017-33116), Spanish Government. AR received funding from the grant PID2019-105769GB-I00 funded by MCIN/AEI/10.13039/50110001103. JRX is further supported by national funds through FCT Foundation for Science and Technology within the scope of UIDB/04423/2020, UIDP/04423/2020 and CEECIND/00577/2018. PER received funding from the Fondo Nacional de Desarrollo Científico, Tecnológico y de Innovación Tecnológica (Fondecyt - Peru): Newton Paulet Researcher Links – Travel Grants [Contract N° 229-2018-FONDECYT] and contract 034-2019-FONDECYT-BM-INC. INV.

Author contributions

ST and AR designed the research. ST, PR, KB, FS, CL, VK, JC, H-TR, CM, JD, FS, JRX, PC and AR collected samples. ST, AR, AM, AC, KB, CW and PER conducted the lab work. PR, JC, JD, AR and PC performed spicule analyses. ST, AR, AM, AC, VT, MBA and CL performed the population genomic analyses. KB and UH performed the microbial community analyses. ST, AM and AR wrote the paper. All authors read and approved the manuscript.

Ethical approval

All applicable international, national, and/or institutional guidelines for the care and use of animals were followed by the authors.

Sampling and field studies

All necessary permits for sampling and observational field studies have been obtained by the authors from the competent authorities and are mentioned in the acknowledgements.

Data accessibility

Sponge *COI* data generated in this study were deposited in GenBank with Accession Numbers MT495710–MT495731, MT506122 –MT506149, and MT506477– MT506490.*16S* amplicon sequences in this study were deposited in the NCBI SRA database, BioProject PRJNA626433. RAD-seq data for each individual sample are deposited in the NCBI SRA database, BioProject PRJNA635421. All other data generated or analysed during this study are included in this published

article and its supplementary information files.

Declaration of competing interest

The authors declare that they have no known competing financial interests or personal relationships that could have appeared to influence the work reported in this paper.

Acknowledgements

We would like to dedicate this article to the memory of Prof. Hans Tore Rapp, who was a wonderful scientist and person and an esteemed member of the sponge community. Thanks are also given to David Rees and Pedro Ribeiro for helping with COI sequencing of some of the specimens. We thank the crew of all the vessels that were involved in sample collection. We are indebted with the staff at the DNA Sequencing Facility, Natural History Museum of London, specially to Elena Lugli, Andie Hall and Claire Griffin, for all the help and support provided. We also thank all the members of the Riesgo Lab, Martín Taboada, Teo Taboada and Otilia Moreno, for all the help they provided during the sample processing and writing of the manuscript. Two anonymous reviewers are also acknowledged for their contribution to an early version of the manuscript.

Appendix A. Supplementary data

Supplementary data to this article can be found online at https://doi.org/10.1016/j.dsr.2021.103685.

References

Akaike, H., 1998. Information Theory and an Extension of the Maximum Likelihood Principle. In: Selected Papers of Hirotugu Akaike. Springer, New York, NY, pp. 199–213. https://doi.org/10.1007/978-1-4612-1694-0_15.

Altschul, S.F., Gish, W., Miller, W., Myers, E.W., Lipman, D.J., 1990. Basic local alignment search tool. J. Mol. Biol. 215, 403–410. https://doi.org/10.1016/S0022-2836(05)80360-2.

Álvarez, B., Hooper, J., 2002. Family Axinellidae Carter, 1875. In: Hooper, J.N.A., van Soest, R.W.M. (Eds.), Systema Porifera: A Guide to the Classification of Sponges. Kluwer Academic/Plenum Publishers, New York, USA, pp. 724–747.

Andrews, K.R., Good, J.M., Miller, M.R., Luikart, G., Hohenlohe, P.A., 2016. Harnessing the power of RADseq for ecological and evolutionary genomics. Nat. Rev. Genet. 17, 81–92. https://doi.org/10.1038/nrg.2015.28.

Arnold, M.L., Fogarty, N.D., 2009. Reticulate evolution and marine organisms: the final frontier? Int. J. Mol. Sci. 10, 3836–3860. https://doi.org/10.3390/ijms10093836.

Baco, A.R., Etter, R.J., Ribeiro, P.A., von der Heyden, S., Beerli, P., Kinlan, B.P., 2016. A synthesis of genetic connectivity in deep-sea fauna and implications for marine reserve design. Mol. Ecol. 25, 3276–3298. https://doi.org/10.1111/mec.13689.

Beazley, L.I., Kenchington, E.L., Murillo, F.J., Sacau, M. del M., 2013. Deep-sea sponge grounds enhance diversity and abundance of epibenthic megafauna in the Northwest Atlantic. ICES J. Mar. Sci. 70, 1471–1490. https://doi.org/10.1093/icesjms/fst124.

Benjamini, Y., Hochberg, Y., 1995. Controlling the False Discovery Rate: a practical and powerful approach to multiple testing. J. R. Stat. Soc. Ser. B 57, 289–300. https://doi.org/10.1111/j.2517-6161.1995.tb02031.x.

Bolyen, E., Rideout, J.R., Dillon, M.R., Bokulich, N.A., Abnet, C.C., Al-Ghalith, G.A., Alexander, H., Alm, E.J., Arumugam, M., Asnicar, F., Bai, Y., Bisanz, J.E., Bittinger, K., Brejnrod, A., Brislawn, C.J., Brown, C.T., Callahan, B.J., Caraballo-Rodríguez, A.M., Chase, J., Cope, E.K., Da Silva, R., Diener, C., Dorrestein, P.C., Douglas, G.M., Durall, D.M., Duvallet, C., Edwardson, C.F., Ernst, M., Estaki, M., Fouquier, J., Gauglitz, J.M., Gibbons, S.M., Gibson, D.L., Gonzalez, A., Gorlick, K., Guo, J., Hillmann, B., Holmes, S., Holste, H., Huttenhower, C., Huttley, G.A., Janssen, S., Jarmusch, A.K., Jiang, L., Kaehler, B.D., Kang, K. Bin, Keefe, C.R., Keim, P., Kelley, S.T., Knights, D., Koester, I., Kosciolek, T., Kreps, J., Langille, M.G. I., Lee, J., Ley, R., Liu, Y.X., Loftfield, E., Lozupone, C., Maher, M., Marotz, C., Martin, B.D., McDonald, D., McIver, L.J., Melnik, A.V., Metcalf, J.L., Morgan, S.C., Morton, J.T., Naimey, A.T., Navas-Molina, J.A., Nothias, L.F., Orchanian, S.B., Pearson, T., Peoples, S.L., Petras, D., Preuss, M.L., Pruesse, E., Rasmussen, L.B., Rivers, A., Robeson, M.S., Rosenthal, P., Segata, N., Shaffer, M., Shiffer, A., Sinha, R., Song, S.J., Spear, J.R., Swafford, A.D., Thompson, L.R., Torres, P.J., Trinh, P., Tripathi, A., Turnbaugh, P.J., Ul-Hasan, S., van der Hooft, J.J.J., Vargas, F., Vázquez-Baeza, Y., Vogtmann, E., von Hippel, M., Walters, W., Wan, Y., Wang, M., Warren, J., Weber, K.C., Williamson, C.H.D., Willis, A.D., Xu, Z.Z., Zaneveld, J.R., Zhang, Y., Zhu, Q., Knight, R., Caporaso, J.G., 2018. Reproducible, interactive, scalable and extensible microbiome data science using QIIME 2. PeerJ 37, 852–857. https://doi.org/10.1038/s41587-019-0209-9.

Bouchemousse, S., Liautard-Haag, C., Bierne, N., Viard, F., 2016. Distinguishing contemporary hybridization from past introgression with postgenomic ancestry-informative SNPs in strongly differentiated Ciona species. Mol. Ecol. 25, 5527–5542. https://doi.org/10.1111/mec.13854.

Boury-Esnault, N., Pansini, M., Uriz, M.J., 1994. Spongiaires bathyaux de la mer d'Alboran et du golfe ibéro-marocain. Mémoires du Muséum Natl. d'Histoire Nat. 160, 1–174e.

Breusing, C., Johnson, S.B., Vrijenhoek, R.C., Young, C.R., 2019. Host hybridization as a potential mechanism of lateral symbiont transfer in deep-sea vesicomyid clams. Mol. Ecol. 28, 4697–4708. https://doi.org/10.1111/mec.15224.

Brown, R.R., Davis, C.S., Leys, S.P., 2017. Clones or clans: the genetic structure of a deep-sea sponge, *Aphrocallistes vastus,* in unique sponge reefs of British Columbia. Canada. Mol. Ecol. 26, 1045–1059. https://doi.org/10.1111/mec.13982.

Brucker, R.M., Bordenstein, S.R., 2012. Speciation by symbiosis. Trends Ecol. Evol. 27, 443–451. https://doi.org/10.1016/j.tree.2012.03.011.

Busch, K., Taboada, S., Riesgo, A., Koutsouveli, V., Ríos, P., Cristobo, J., Franke, A., Getzlaff, K., Schmidt, C., Biastoch, A., Hentschel, U., 2020. Population connectivity of fan-shaped sponge holobionts in the deep Cantabrian Sea. Deep-Sea Res. Part I Oceanogr. Res. Pap., 103427 https://doi.org/10.1016/j.dsr.2020.103427.

Callahan, B.J., McMurdie, P.J., Rosen, M.J., Han, A.W., Johnson, A.J.A., Holmes, S.P., 2016. DADA2: high-resolution sample inference from Illumina amplicon data. Nat. Methods 13, 581–583. https://doi.org/10.1038/nmeth.3869.

Caporaso, J.G., Lauber, C.L., Walters, W.A., Berg-Lyons, D., Lozupone, C.A., Turnbaugh, P.J., Fierer, N., Knight, R., 2011. Global patterns of 16S rRNA diversity at a depth of millions of sequences per sample. Proc. Natl. Acad. Sci. U. S. A. 108 (Suppl. l), 4516–4522. https://doi.org/10.1073/pnas.1000080107.

Carvalho, M.S., Desqueyroux-Faúndez, R., Hajdu, E., 2007. *Phakellia sur* sp. nov. (Demospongiae, Halichondrida, Axinellidae) from the lower slope off Cape Horn (South America), with a revision of the genus. Mar. Biol. Res. 3, 109–116. https://doi.org/10.1080/17451000701276063.

Castrillejo, M., Casacuberta, N., Christl, M., Vockenhuber, C., Synall, H.A., García-Ibáñez, M.I., Lherminier, P., Sarthou, G., Garcia-Orellana, J., Masqué, P., 2018. Tracing water masses with 129I and 236U in the subpolar North Atlantic along the GEOTRACES GA01 section. Biogeosciences 15, 5545–5564. https://doi.org/10.5194/bg-15-5545-2018.

Catchen, J., Hohenlohe, P.A., Bassham, S., Amores, A., Cresko, W.A., 2013. Stacks: an analysis tool set for population genomics. Mol. Ecol. 22, 3124–3140. https://doi.org/10.1111/mec.12354.

Chaves-Fonnegra, A., Feldheim, K.A., Secord, J., Lopez, J.V., 2015. Population structure and dispersal of the coral-excavating sponge *Cliona delitrix*. Mol. Ecol. 24, 1447–1466. https://doi.org/10.1111/mec.13134.

Clague, G.E., Jones, W.J., Paduan, J.B., Clague, D.A., Vrijenhoek, R.C., 2012. Phylogeography of Acesta clams from submarine seamounts and escarpments along the Western margin of North America. Mar. Ecol. 33, 75–87. https://doi.org/10.1111/j.1439-0485.2011.00458.x.

Clement, M., Posada, D., Crandall, K., 2000. TCS: a computer program to estimate gene genealogies. Mol. Ecol. 9, 1657–1659.

Combosch, D.J., Lemer, S., Ward, P.D., Landman, N.H., Giribet, G., 2017. Genomic signatures of evolution in Nautilus —an endangered living fossil. Mol. Ecol. 26, 5923–5938. https://doi.org/10.1111/mec.14344.

Cranston, A., Taboada, S., Koutsouveli, V., Schuster, A., Riesgo, A., 2021. A population specific mitochondrial intron from the sponge Phakellia robusta in the North-East Atlantic. Deep-Sea Res. Part I Oceanogr. Res. Pap. 172, 103534 https://doi.org/10.1016/j.dsr.2021.103534.

Dailianis, T., Tsigenopoulos, C.S., Dounas, C., Voultsiadou, E., 2011. Genetic diversity of the imperilled bath sponge *Spongia officinalis* Linnaeus, 1759 across the Mediterranean Sea: patterns of population differentiation and implications for taxonomy and conservation. Mol. Ecol. 20, 3757–3772. https://doi.org/10.1111/j.1365-294X.2011.05222.x.

Darriba, D., Taboada, G.L., Doallo, R., Posada, D., 2012. jModelTest 2: more models, new heuristics and parallel computing. Nat. Methods 9. https://doi.org/10.1038/nmeth.2109, 772–772.

De Goeij, J.M., Van Oevelen, D., Vermeij, M.J.A., Osinga, R., Middelburg, J.J., De Goeij, A.F.P.M., Admiraal, W., 2013. Surviving in a marine desert: the sponge loop retains resources within coral reefs. Science (80-.) 342, 108–110. https://doi.org/10.1126/science.1241981.

Earl, D.A., vonHoldt, B.M., 2012. Structure HARVESTER: a website and program for visualizing STRUCTURE output and implementing the Evanno method. Conserv. Genet. Resour. 4, 359–361. https://doi.org/10.1007/s12686-011-9548-7.

EC, 2013. Interpretation Manual of European Union Habitats. EUR28. European Commision DG Environment.

Ennos, R.A., French, G.C., Hollingsworth, P.M., 2005. Conserving taxonomic complexity. Trends Ecol. Evol. 20, 164–168. https://doi.org/10.1016/j.tree.2005.01.012.

Erwin, P.M., López-Legentil, S., González-Pech, R., Turon, X., 2012. A specific mix of generalists: bacterial symbionts in Mediterranean *Ircinia* spp. FEMS Microbiol. Ecol. 79, 619–637. https://doi.org/10.1111/j.1574-6941.2011.01243.x.

Excoffier, L., Lischer, H.E.L., 2010. Arlequin suite ver 3.5: a new series of programs to perform population genetics analyses under Linux and Windows. Mol. Ecol. Resour. 10, 564–567. https://doi.org/10.1111/j.1755-0998.2010.02847.x.

Folmer, O., Black, M., Hoeh, W., Lutz, R., Vrijenhoek, R., 1994. DNA primers for amplification of mitochondrial cytochrome c oxidase subunit I from diverse metazoan invertebrates. Mol. Mar. Biol. Biotechnol. 3, 294–299. https://doi.org/10.1371/journal.pone.0013102.

Fourt, M., Goujard, A., Pérez, T., Chevaldonné, P., 2017. Guide de la faune profonde de la mer Méditerranée. Explorations des roches et des canyons sous-marins des côtes françaises. Patrimoines naturels. Publ. Sci. du Museum Natl. d'Histoire Nat. Paris 75, 1–184.

Fraïsse, C., Belkhir, K., Welch, J.J., Bierne, N., 2016. Local interspecies introgression is the main cause of extreme levels of intraspecific differentiation in mussels. Mol. Ecol. 25, 269–286. https://doi.org/10.1111/mec.13299.

France, S.C., Kocher, T.D., 1996. Geographic and bathymetric patterns of mitochondrial 16S rRNA sequence divergence among deep-sea amphipods, *Eurythenes gryllus*. Mar. Biol. 126, 633–643. https://doi.org/10.1007/BF00351330.

Galaska, M.P., Sands, C.J., Santos, S.R., Mahon, A.R., Halanych, K.M., 2017. Geographic structure in the Southern Ocean circumpolar brittle star *Ophionotus victoriae* (Ophiuridae) revealed from mtDNA and single-nucleotide polymorphism data. Ecol. Evol. 7, 475–485. https://doi.org/10.1002/ece3.2617.

Gloeckner, V., Wehrl, M., Moitinho-Silva, L., Gernert, C., Hentschel, U., Schupp, P., Pawlik, J.R., Lindquist, N.L., Erpenbeck, D., Wörheide, G., Wörheide, G., 2014. The HMA-LMA dichotomy revisited: an electron microscopical survey of 56 sponge species. Biol. Bull. 227, 78–88. https://doi.org/10.1086/BBLv227n1p78.

Hansen, B., Østerhus, S., 2000. North Atlantic-nordic seas exchanges. Prog. Oceanogr. 45, 109–208. https://doi.org/10.1016/S0079-6611(99)00052-X.

Harper, F.M., Hart, M.W., 2007. Morphological and phylogenetic evidence for hybridization and introgression in a sea star secondary contact zone. Invertebr. Biol. 126, 373–384. https://doi.org/10.1111/j.1744-7410.2007.00107.x.

Hentschel, U., Piel, J., Degnan, S.M., Taylor, M.W., 2012. Genomic insights into the marine sponge microbiome. Nat. Rev. Microbiol. 10, 641–654. https://doi.org/10.1038/nrmicro2839.

Hentschel, U., Usher, K.M., Taylor, M.W., 2006. Marine sponges as microbial fermenters. FEMS Microbiol. Ecol. 55, 167–177. https://doi.org/10.1111/j.1574-6941.2005.00046.x.

Heredia, B., Pantoja, J., Tejedor, A., Sánchez, F., 2008. La primera gran área marina protegida en españa: El Cachucho, un oásis de vida en el Cantábrico. Ambient. La Rev. del Minist. Medio Ambient. 76, 10–17.

Hohenlohe, P.A., Amish, S.J., Catchen, J.M., Allendorf, F.W., Luikart, G., 2011. Next-generation RAD sequencing identifies thousands of SNPs for assessing hybridization between rainbow and westslope cutthroat trout. Mol. Ecol. Resour. 11, 117–122. https://doi.org/10.1111/j.1755-0998.2010.02967.x.

Hohenlohe, P.A., Hand, B.K., Andrews, K.R., Luikart, G., 2018. Population Genomics Provides Key Insights in Ecology and Evolution. In: Rajora, O.P. (Ed.), Population Genomics: : Concepts, Approaches and Applications, pp. 483–510. https://doi.org/10.1007/13836_2018_20.

Howell, K.L., Piechaud, N., Downie, A.L., Kenny, A., 2016. The distribution of deep-sea sponge aggregations in the North Atlantic and implications for their effective spatial management. Deep. Res. Part I Oceanogr. Res. Pap. 115, 309–320. https://doi.org/10.1016/j.dsr.2016.07.005.

Huang, D., Meier, R., Todd, P.A., Chou, L.M., 2008. Slow mitochondrial COI sequence evolution at the base of the metazoan tree and its implications for DNA barcoding. J. Mol. Evol. 66, 167–174. https://doi.org/10.1007/s00239-008-9069-5.

Hughes, D.J., Narayanaswamy, B.E., 2013. Impacts of climate change on deep-sea habitats. MCCIP Sci. Rev. 204–210. https://doi.org/10.14465/2013.arc21.204-210.

Jakobsson, M., Rosenberg, N.A., 2007. CLUMPP: a cluster matching and permutation program for dealing with label switching and multimodality in analysis of population structure. Bioinformatics 23, 1801–1806. https://doi.org/10.1093/bioinformatics/btm233.

Jeffries, D.L., Copp, G.H., Handley, L.L., Håkan Olsén, K., Sayer, C.D., Hänfling, B., 2016. Comparing RADseq and microsatellites to infer complex phylogeographic patterns, an empirical perspective in the Crucian carp, *Carassius carassius*. L. Mol. Ecol. 25, 2997–3018. https://doi.org/10.1111/mec.13613.

Jombart, T., Devillard, S., Balloux, F., 2010. Discriminant analysis of principal components: a new method for the analysis of genetically structured populations. BMC Genet. 11, 94. https://doi.org/10.1186/1471-2156-11-94.

Katoh, K., Standley, D.M., 2013. MAFFT Multiple sequence alignment software version 7: improvements in performance and usability. Mol. Biol. Evol. 30, 772–780. https://doi.org/10.1093/molbev/mst010.

Kearse, M., Moir, R., Wilson, A., Stones-Havas, S., Cheung, M., Sturrock, S., Buxton, S., Cooper, A., Markowitz, S., Duran, C., Thierer, T., Ashton, B., Meintjes, P., Drummond, A., 2012. Geneious Basic: an integrated and extendable desktop software platform for the organization and analysis of sequence data. Bioinformatics 28, 1647–1649. https://doi.org/10.1093/bioinformatics/bts199.

Kenchington, E., Power, D., Koen-Alonso, M., 2013. Associations of demersal fish with sponge grounds on the continental slopes of the northwest Atlantic. Mar. Ecol. Prog. Ser. 477, 217–230. https://doi.org/10.3354/meps10127.

Klitgaard, A.B., 1995. The fauna associated with outer shelf and upper slope sponges (porifera, demospongiae) at the Faroe Islands, northeastern Atlantic. Sarsia 80, 1–22. https://doi.org/10.1080/00364827.1995.10413574.

Kozich, J.J., Westcott, S.L., Baxter, N.T., Highlander, S.K., Schloss, P.D., 2013. Development of a dual-index sequencing strategy and curation pipeline for analyzing amplicon sequence data on the miseq illumina sequencing platform. Appl. Environ. Microbiol. 79, 5112–5120. https://doi.org/10.1128/AEM.01043-13.

Kumar, S., Stecher, G., Li, M., Knyaz, C., Tamura, K., 2018. Mega X: molecular evolutionary genetics analysis across computing platforms. Mol. Biol. Evol. 35, 1547–1549. https://doi.org/10.1093/molbev/msy096.

Leigh, J.W., Bryant, D., 2015. Popart : full-feature software for haplotype network construction. Methods Ecol. Evol. 6, 1110–1116. https://doi.org/10.1111/2041-210X.12410.

Leiva, C., Taboada, S., Kenny, N.J., Combosch, D., Giribet, G., Jombart, T., Riesgo, A., 2019. Population substructure and signals of divergent adaptive selection despite admixture in the sponge Dendrilla Antarctica from shallow waters surrounding the Antarctic Peninsula. Mol. Ecol. 28, 3151–3170. https://doi.org/10.1111/mec.15135.

Letunic, I., Bork, P., 2016. Interactive tree of life (iTOL) v3: an online tool for the display and annotation of phylogenetic and other trees. Nucleic Acids Res. 44, W242–W245. https://doi.org/10.1093/nar/gkw290.

Lozupone, C., Knight, R., 2005. UniFrac: a new phylogenetic method for comparing microbial communities. Appl. Environ. Microbiol. 71, 8228–8235. https://doi.org/10.1128/AEM.71.12.8228-8235.2005.

Maldonado, M., Aguilar, R., Bannister, R.J., James, J., Conway, K.W., Dayton, P.K., Cristina, D., Gutt, J., Kelly, M., Kenchington, E.L.R., Leys, S.P., Shirley, A., Tendal, O. S., Rapp, H.T., Klaus, R., Young, C.M., 2017. Sponge Grounds as Key Marine Habitats: A Synthetic Review of Types, Structure, Functional Roles, and Conservation Concerns. In: Marine Animal Forests: the Ecology of Benthic Biodiversity Hotspots, pp. 145–183. https://doi.org/10.1007/978-3-319-21012-4.

Maldonado, M., Riesgo, A., 2009. Reproduction in Porifera: a synoptic overview. Treballs la Soc. Catalana Biol. 59, 29–49. https://doi.org/10.2436/20.1501.02.56.

Malinsky, M., Trucchi, E., Lawson, D.J., Falush, D., 2018. RADpainter and fineRADstructure: population inference from RADseq data. Mol. Biol. Evol. 35, 1284–1290. https://doi.org/10.1093/molbev/msy023.

Manni, F., Guerard, E., Heyer, E., 2004. Geographic patterns of (genetic, morphologic, linguistic) variation: how barriers can be detected by using Monmonier's algorithm. Hum. Biol. 76, 173–190. https://doi.org/10.1353/hub.2004.0034.

Margulis, L., Dorion, S., 2008. Acquiring Genomes: A Theory of the Origin of Species. Basic Books.

McFall-Ngai, M., Hadfield, M.G., Bosch, T.C.G., Carey, H.V., Domazet-Lošo, T., Douglas, A.E., Dubilier, N., Eberl, G., Fukami, T., Gilbert, S.F., Hentschel, U., King, N., Kjelleberg, S., Knoll, A.H., Kremer, N., Mazmanian, S.K., Metcalf, J.L., Nealson, K., Pierce, N.E., Rawls, J.F., Reid, A., Ruby, E.G., Rumpho, M., Sanders, J. G., Tautz, D., Wernegreen, J.J., 2013. Animals in a bacterial world, a new imperative for the life sciences. Proc. Natl. Acad. Sci. U. S. A. 110, 3229–3236. https://doi.org/10.1073/pnas.1218525110.

Meirmans, P.G., Van Tienderen, P.H., 2004. GENOTYPE and GENODIVE: two programs for the analysis of genetic diversity of asexual organisms. Mol. Ecol. Notes 4, 792–794. https://doi.org/10.1111/j.1471-8286.2004.00770.x.

Morrow, C.C., Picton, B.E., Erpenbeck, D., Boury-Esnault, N., Maggs, C.A., Allcock, A.L., 2012. Congruence between nuclear and mitochondrial genes in Demospongiae: a new hypothesis for relationships within the G4 clade (Porifera: Demospongiae). Mol. Phylogenet. Evol. 62, 174–190. https://doi.org/10.1016/j.ympev.2011.09.016.

Morrow, C.C., Redmond, N.E., Picton, B.E., Thacker, R.W., Collins, A.G., Maggs, C.A., Sigwart, J.D., Allcock, A.L., 2013. Molecular phylogenies support homoplasy of multiple morphological characters used in the taxonomy of heteroscleromorpha (Porifera: Demospongiae). Integr. Comp. Biol. 53, 428–446. https://doi.org/10.1093/icb/ict065.

Müllner, D., 2013. Fastcluster: fast hierarchical, agglomerative clustering routines for R and Python. J. Stat. Software 53, 1–18. https://doi.org/10.18637/jss.v053.i09.

Muyzer, G., De Waal, E.C., Uitterlinden, A.G., 1993. Profiling of complex microbial populations by denaturing gradient gel electrophoresis analysis of polymerase chain reaction-amplified genes coding for 16S rRNA. Appl. Environ. Microbiol. 59, 1–6. https://doi.org/10.1128/aem.59.3.695-700.1993.

O'Hara, T.D., England, P.R., Guasekera, R.M., Naughton, K.M., 2014. Limited phylogeographic structure for five bathyal ophiuroids at continental scales. Deep-Sea Res. Part I Oceanogr. Res. Pap. 84, 18–28. https://doi.org/10.1016/J.DSR.2013.09.009.

Pante, E., Puillandre, N., Viricel, A., Arnaud-Haond, S., Aurelle, D., Castelin, M., Chenuil, A., Destombe, C., Forcioli, D., Valero, M., Viard, F., Samadi, S., 2015. Species are hypotheses: avoid connectivity assessments based on pillars of sand. Mol. Ecol. 24, 525–544. https://doi.org/10.1111/mec.13048.

Paoli, C., Montefalcone, M., Morri, C., Vassallo, P., Nike Bianchi, C., 2017. Ecosystem functions and services of the marine animal forests. In: Marine Animal Forests: the Ecology of Benthic Biodiversity Hotspots, pp. 1271–1312. https://doi.org/10.1007/978-3-319-21012-4.

Paris, J.R., Stevens, J.R., Catchen, J.M., 2017. Lost in parameter space: a road map for stacks. Methods Ecol. Evol. 8, 1360–1373. https://doi.org/10.1111/2041-210X.12775.

Pérez-Portela, R., Noyer, C., Becerro, M.A., 2015. Genetic structure and diversity of the endangered bath sponge *Spongia lamella*. Aquat. Conserv. Mar. Freshw. Ecosyst. 25, 365–379. https://doi.org/10.1002/aqc.2423.

Pérez-Portela, R., Riesgo, A., 2018. Population Genomics of Early-Splitting Lineages of Metazoans 1–35. https://doi.org/10.1007/13836_2018_13.

Peterson, B.K., Weber, J.N., Kay, E.H., Fisher, H.S., Hoekstra, H.E., 2012. Double digest RADseq: an inexpensive method for de novo SNP discovery and genotyping in model and non-model species. PLoS One 7, e37135. https://doi.org/10.1371/journal.pone.0037135.

Pham, C.K., Murillo, F.J., Lirette, C., Maldonado, M., Colaço, A., Ottaviani, D., Kenchington, E., 2019. Removal of deep-sea sponges by bottom trawling in the Flemish Cap area: conservation, ecology and economic assessment. Sci. Rep. 9, 1–13. https://doi.org/10.1038/s41598-019-52250-1.

Pham, C.K., Vandeperre, F., Menezes, G., Porteiro, F., Isidro, E., Morato, T., 2015. The importance of deep-sea vulnerable marine ecosystems for demersal fish in the Azores. Deep-Sea Res. Part I Oceanogr. Res. Pap. 96, 80–88. https://doi.org/10.1016/J.DSR.2014.11.004.

Pita, L., Rix, L., Slaby, B.M., Franke, A., Hentschel, U., 2018. The Sponge Holobiont in a Changing Ocean : from Microbes to Ecosystems, pp. 1–18.

Pöppe, J., Sutcliffe, P., Hooper, J.N.A., Wörheide, G., Erpenbeck, D., 2010. CO I barcoding reveals new clades and radiation patterns of indo-pacific sponges of the family irciniidae (Demospongiae: dictyoceratida). PLoS One 5, e9950. https://doi.org/10.1371/journal.pone.0009950.

Pritchard, J.K., Stephens, M., Donnelly, P., 2000. Inference of population structure using multilocus genotype data. Genetics 155, 954–959.
Quast, C., Pruesse, E., Yilmaz, P., Gerken, J., Schweer, T., Yarza, P., Peplies, J., Glöckner, F.O., 2013. The SILVA ribosomal RNA gene database project: improved data processing and web-based tools. Nucleic Acids Res. 41, 590–596. https://doi.org/10.1093/nar/gks1219.
Quattro, J., Chase, M., Rex, M., Greig, T., Etter, R., 2001. Extreme mitochondrial DNA divergence within populations of the deep-sea gastropod Frigidoalvania brychia. Mar. Biol. 139, 1107–1113. https://doi.org/10.1007/s002270100662.
Rambaut, A., 2014. FigTree. V. 1.4. 2 Software. Inst. Evol. Biol. Univ., Edinburgh.
Riesgo, A., Perez-Portela, R., Pita, L., Blasco, G., Erwin, P.M., Lopez-Legentil, S., 2016. Population structure and connectivity in the Mediterranean sponge *Ircinia fasciculata* are affected by mass mortalities and hybridization. Heredity (Edinb). https://doi.org/10.1038/hdy.2016.41.
Riesgo, A., Taboada, S., Pérez-Portela, R., Melis, P., Xavier, J.R., Blasco, G., López-legentil, S., 2019. Genetic diversity , connectivity and gene flow along the distribution of the emblematic Atlanto-Mediterranean sponge *Petrosia ficiformis* (Haplosclerida , Demospongiae). BMC Evol. Biol. 19, 24. https://doi.org/10.1186/s12862-018-1343-6.
Roberts, C.M., 2002. Deep impact: the rising toll of fishing in the deep sea. Trends Ecol. Evol. 17, 242–245. https://doi.org/10.1016/S0169-5347(02)02492-8.
Rodríguez-Basalo, A., Sánchez, F., Punzón, A., Gómez-Ballesteros, M., 2019. Updating the master management plan for el Cachucho MPA (Cantabrian Sea) using a spatial planning approach. Continent. Shelf Res. 184, 54–65. https://doi.org/10.1016/j.csr.2019.06.010.
Roesti, M., Salzburger, W., Berner, D., 2012. Uninformative polymorphisms bias genome scans for signatures of selection. BMC Evol. Biol. 12 https://doi.org/10.1186/1471-2148-12-94.
Sánchez, F., Rodríguez Basalo, A., García-Alegre, A., Gómez-Ballesteros, M., 2017. Hard-bottom bathyal habitats and keystone epibenthic species on le danois bank (Cantabrian Sea). J. Sea Res. 130, 134–153. https://doi.org/10.1016/j.seares.2017.09.005.
Santín, A., Grinyó, J., Ambroso, S., Uriz, M.-J., Gori, A., Dominguez-Carrió, C., Gili, J.-M., 2018. Sponge assemblages on the deep mediterranean continental shelf and slope (menorca channel, Western Mediterranean Sea). Deep-Sea Res. Part I Oceanogr. Res. Pap. 131, 75–86.
Schüller, M., 2011. Evidence for a role of bathymetry and emergence in speciation in the genus *Glycera* (Glyceridae, polychaeta) from the deep Eastern Weddell sea. Polar Biol. 34, 549–564. https://doi.org/10.1007/s00300-010-0913-x.
Seehausen, O., Butlin, R.K., Keller, I., Wagner, C.E., Boughman, J.W., Hohenlohe, P.A., Peichel, C.L., Saetre, G.P., Bank, C., Brännström, Å., Brelsford, A., Clarkson, C.S., Eroukhmanoff, F., Feder, J.L., Fischer, M.C., Foote, A.D., Foote, A.D., Franchini, P., Jiggins, C.D., Jones, F.C., Lindholm, A.K., Lucek, K., Maan, M.E., Marques, D.A., Marques, D.A., Martin, S.H., Matthews, B., Meier, J.I., Meier, J.I., Möst, M., Möst, M., Nachman, M.W., Nonaka, E., Rennison, D.J., Schwarzer, J., Schwarzer, J., Schwarzer, J., Watson, E.T., Westram, A.M., Widmer, A., 2014. Genomics and the origin of species. Nat. Rev. Genet. 15, 176–192. https://doi.org/10.1038/nrg3644.
Segata, N., Izard, J., Waldron, L., Gevers, D., Miropolsky, L., Garrett, W.S., Huttenhower, C., 2011. Metagenomic biomarker discovery and explanation. Genome Biol. 12, R60. https://doi.org/10.1186/gb-2011-12-6-r60.
Spielman, D., Brook, B.W., Frankham, R., 2004. Most species are not driven to extinction before genetic factors impact them, 101, 15261–15264.
Stamatakis, A., 2014. RAxML version 8: a tool for phylogenetic analysis and post-analysis of large phylogenies. Bioinformatics 30, 1312–1313. https://doi.org/10.1093/bioinformatics/btu033.
Storesund, J.E., Sandaa, R.A., Thingstad, T.F., Asplin, L., Albretsen, J., Erga, S.R., 2017. Linking bacterial community structure to advection and environmental impact along a coast-fjord gradient of the Sognefjord, western Norway. Prog. Oceanogr. 159, 13–30. https://doi.org/10.1016/j.pocean.2017.09.002.
Sundqvist, L., Keenan, K., Zackrisson, M., Prodöhl, P., Kleinhans, D., 2016. Directional genetic differentiation and relative migration. Ecol. Evol. 6, 3461–3475. https://doi.org/10.1002/ece3.2096.
Sweetman, A.K., Thurber, A.R., Smith, C.R., Levin, L.A., Mora, C., Wei, C.-L., Gooday, A.J., Jones, D.O.B., Rex, M., Yasuhara, M., Ingels, J., Ruhl, H.A., Frieder, C.A., Danovaro, R., Würzberg, L., Baco, A., Grupe, B.M., Pasulka, A., Meyer, K.S., Dunlop, K.M., Henry, L.-A., Roberts, J.M., 2017. Major impacts of climate change on deep-sea benthic ecosystems. Elem Sci Anth 5, 4. https://doi.org/10.1525/elementa.203.
Taboada, S., Riesgo, A., Wiklund, H., Paterson, G.L.J., Koutsouveli, V., Santodomingo, N., Dale, A.C., Smith, C.R., Jones, D.O.B., Dahlgren, T.G., Glover, A.G., 2018. Implications of population connectivity studies for the design of marine protected areas in the deep sea: an example of a demosponge from the Clarion-Clipperton Zone. Mol. Ecol. 27, 4657–4679. https://doi.org/10.1111/mec.14888.
Taylor, M.L., Roterman, C.N., 2017. Invertebrate population genetics across Earth's largest habitat: the deep-sea floor. Mol. Ecol. 26, 4872–4896. https://doi.org/10.1111/mec.14237.
Thomas, T., Moitinho-Silva, L., Lurgi, M., Björk, J.R., Easson, C., Astudillo-García, C., Olson, J.B., Erwin, P.M., López-Legentil, S., Luter, H., Chaves-Fonnegra, A., Costa, R., Schupp, P.J., Steindler, L., Erpenbeck, D., Gilbert, J., Knight, R., Ackermann, G., Victor Lopez, J., Taylor, M.W., Thacker, R.W., Montoya, J.M., Hentschel, U., Webster, N.S., 2016. Diversity, structure and convergent evolution of the global sponge microbiome. Nat. Commun. 7, 11870 https://doi.org/10.1038/ncomms11870.
Topsent, E., 1928. Spongiaires de l'Atlantique et de la Méditerranée provenant des croisières du Prince Albert I de Monaco. 74: Résultats des campagnes Sci. Accompl. par le Prince Albert I. Monaco 74, 1–376 pls I–XI).
Topsent, E., 1892. Contribution à l'étude des Spongiaires de l'Atlantique Nord (Golfe de Gascogne, Terre-Neuve, Açores). Résultats des campagnes Sci. Accompl. par le Prince Albert I. Monaco 2 1–165 (pls I–XI).
Topsent, E., 1890. Notice préliminaire sur les spongiaires recueillis durant les campagnes de l'Hirondelle. Bull. la Société Zool. Fr. 15, 65–71.
Uriz, M.-J., 1984. Material para la fauna de esponjas ibéricas: nuevas senalizaciones de Demosponjas en nuestras costas. Actas do IV Simp. ibérico Estud. do benthos Mar. 3, 131–140.
Van Soest, R.W.M., Boury-Esnault, N., Hooper, J.N.A., Rützler, K., de Voogd, N.J., Alvarez, B., Hajdu, E., Pisera, A.B., Manconi, R., Schönberg, C., Klautau, M., Kelly, M., Vacelet, J., Dohrmann, M., Díaz, M.-C., Cárdenas, P., Carballo, J.L., Ríos, P., Do, C.C., 2020. World Porifera Database. Accessed at ([WWW Document]). http://www.marinespecies.org/porifera on 2020-04-13.
Webster, N.S., Taylor, M.W., Behnam, F., Lücker, S., Rattei, T., Whalan, S., Horn, M., Wagner, M., 2010. Deep sequencing reveals exceptional diversity and modes of transmission for bacterial sponge symbionts. Environ. Microbiol. 12, 2070–2082. https://doi.org/10.1111/j.1462-2920.2009.02065.x.
Wedding, L.M., Reiter, S.M., Smith, C.R., Gjerde, K.M., Kittinger, J.N., Friedlander, A.M., Gaines, S.D., Clark, M.R., Thurnherr, A.M., Hardy, S.M., Crowder, L.B., 2015. Managing mining of the deep seabed. Science (80-.) 349, 144–145. https://doi.org/10.1126/science.aac6647.
Willis, B.L., van Oppen, M.J.H., Miller, D.J., Vollmer, S.V., Ayre, D.J., 2006. The role of hybridization in the evolution of reef corals. Annu. Rev. Ecol. Evol. Syst. 37, 489–517. https://doi.org/10.1146/annurev.ecolsys.37.091305.110136.
Witte, U., 1996. Seasonal reproduction in deep-sea sponges - triggered by vertical particle flux? Mar. Biol. 124, 571–581. https://doi.org/10.1007/BF00351038.
Won, Y., Hallam, S.J., O'Mullan, G.D., Vrijenhoek, R.C., 2003. Cytonuclear disequilibrium in a hybrid zone involving deep-sea hydrothermal vent mussels of the genus *Bathymodiolus*. Mol. Ecol. 12, 3185–3190. https://doi.org/10.1046/j.1365-294X.2003.01974.x.
Young, C.M., Devin, M.G., Jaeckle, W.B., Ekaratne, S., George, S.B., 1996. The potential for ontogenetic vertical migration by larvae of bathyal echinoderms. Oceanol. Acta 19, 263–271.
Zardus, J.D., Etter, R.J., Chase, M.R., Rex, M.A., Boyle, E.E., 2006. Bathymetric and geographic population structure in the pan-Atlantic deep-sea bivalve *Deminucula atacellana* (Schenck, 1939). Mol. Ecol. 15, 639–651. https://doi.org/10.1111/j.1365-294X.2005.02832.x.